Exploration and Mining Geology, Vol. 15, Nos. 3–4, p. 241–261, 2006

0964-1823/00 $17.00 + .00

Chemostratigraphy of Volcanic Rocks Hosting Massive Sulfide Clasts Within the Meductic Group, West-Central New Brunswick

S.H. McCLENAGHAN[1], D.R. LENTZ[1], AND L.R. FYFFE[2]

(Received April 21, 2002; accepted April 21, 2006)

Abstract — The Eel River area in the southwestern Miramichi terrane of New Brunswick contains a complete calc-alkaline suite of volcanic rocks that are interlayered with intervals of sedimentary and polylithic fragmental rocks, and are overlain by a thick sedimentary sequence. This package, collectively referred to as the Meductic Group, was deposited in a submerged volcanic arc setting interpreted to be part of the Popelogan arc. Rifting of this arc led to the development of the Tetagouche-Exploits back-arc basin, and formation of volcanogenic massive sulfide deposits in bimodal volcanic rocks of the Bathurst Mining Camp in the northeastern Miramichi Terrane. Unlike the Bathurst Mining Camp, volcanic rocks in the southeastern Miramichi Highlands form a continuous calc-alkaline suite characterized by increasing Zr/TiO_2 with increasing SiO_2, in part resulting from progressive coupled assimilation and fractional crystallization of nested magma systems. Slumping of semi-consolidated volcanic and sedimentary rocks in topographically unstable areas resulted in numerous slumps and debris flows that are preserved throughout the Eel River area.

In the early 1990s, the discovery of a large sulfide clast in a road cut along the Benton road sparked interest in the volcanogenic massive sulfide potential of the Eel River area. Subsequent drilling intersected smaller fragments, one clast of which graded 16.7% Zn, 5.6% Pb, 90 ppm Ag, and 220 ppb Au. The intersection of thin lenses of stratiform sulfides in another drillhole indicates favorable conditions for the preservation of massive sulfides. Their subsequent incorporation into synvolcanic debris flows resulted in the transport and deposition of sulfide clasts from hydrothermal vents to more distal locations. Similar to the Buchans deposits of Newfoundland, tracing these debris flows back to their source would be beneficial from an exploration perspective. Approximately 15 km to the southwest of the Eel River area, gold-bearing base metal sulfide clasts (11.1% Zn, 6.13% Pb, 0.19% Cu, 108 ppm Ag, and 1100 ppb Au) occur within intermediate-composition volcanic rocks at Monument Brook in eastern Maine.

Key Words: Massive sulfide clast, Debris flow, Chemostratigraphy, Volcanic rocks, Eel River, Meductic Group.

Sommaire — Le secteur d'Eel River dans le sud-ouest de la terrane de Miramichi au Nouveau Brunswick contient une séquence complète de roches volcaniques calco-alcalines interstratifiées avec des roches sédimentaires et fragmentaires polylithologiques, sous une épaisse couverture sédimentaire. Cet assemblage constitue le Groupe de Meductic, et a été déposé dans un environnement d'arc insulaire interprété comme une partie de l'arc de Popelogan. Le rifting de cet arc à mené au développement du bassin d'arrière-arc de Tetagouche-Exploits, et à la formation de gisements de sulfures massifs volcanogènes dans les roches volcaniques bimodales du Camp Minier de Bathurst dans le nord-est de la terrane de Miramichi. Contrairement au Camp Minier de Bathurst, les roches volcaniques des hautes terres du sud-est de Miramichi constituent une suite calco-alcaline continue caractérisée par un accroissement du rapport Zr/TiO_2 à des valeurs croissantes de SiO_2, résultant en partie de l'assimilation progressive et de la cristallisation fractionnée de systèmes magmatiques superposés. L'effondrement de roches volcaniques et sédimentaires semi-consolidées dans des secteurs topographiquement instables est à l'origine des nombreux slumps et coulées de débris qui sont préservés dans le secteur d'Eel River.

Au début des années 1990, la découverte d'un large claste de sulfures le long de la route Benton provoqué un intérêt pour le potentiel en gisements de sulfures massifs volcanogènes dans les secteur d'Eel River. Des forages ont par la suite recoupé des fragments plus petits, dont un claste qui a retourné des teneurs de 16.7% Zn, 5.6% Pb, 90 ppm Ag et 220 ppb Au. Le recoupement de minces lentilles de sulfures stratiformes dans un autre forage indique des conditions propices à la préservation des sulfures massifs. Leur incorporation subséquente dans des coulées de débris synvolcaniques est responsable du transport et de la déposition de ces clastes de sulfures depuis les évents hydrothermaux jusqu'à des endroits plus distaux. Ces coulées de débris sont similaires aux gisements de Buchans à Terre-Neuve, et les tracer jusqu'à leur source serait bénéfique du point de vue de l'exploration. Environ 15 km au sud-ouest du secteur d'Eel River, des clastes aurifères de sulfures de métaux usuels (11.1% Zn, 6.13% Pb, 0.19% Cu, 108 ppm Ag, et 1100 ppb Au) sont présents dans des roches volcaniques de composition intermédiaire à Monument Brook, dans l'est du Maine.

[1] Department of Geology, University of New Brunswick, P.O. Box 4400, Fredericton, New Brunswick, E3B 5A3.
[2] Geological Surveys Branch, New Brunswick Department of Natural Resources and Energy, P.O. Box 6000, Fredericton, New Brunswick, E3B 5H1.

Introduction

The Eel River area (Fig. 1) is located south of Benton in western New Brunswick, Canada. During the early 1990s, the Eel River area was the focus of exploration following the discovery, in a road cut along the Benton road, of a large sulfide clast (Fig. 2a) hosted by Ordovician volcanic rocks of the Meductic Group. This discovery prompted BHP Minerals Canada Ltd. to drill 12 holes along the strike of this belt of volcanic rocks in order to determine the extent of mineralization (Williamson, 1996); unfortunately, only minor exhalative sulfides and sulfide breccia were intersected (Fig. 2b). Several pyrrhotite-rich clasts (>10 cm) occur in drillhole BB 92-2, one of which grades 16.7% Zn, 5.6% Pb, 90 ppm Ag, and 220 ppb Au (Williamson, 1996). A one-meter mineralized section containing 60% pyrite was intersected in DDH BB 94-7 (Williamson, 1996); however, the base and precious-metal contents of these sulfides are uniformly low (17 ppm Pb+Zn, 200 ppm Cu, and 11 ppb Au). Gold-bearing base metal massive sulfide clasts (11.1% Zn, 6.13% Pb, 0.19% Cu, 108 ppm Ag, and 1100 ppb Au) also occur in intermediate-composition volcanic rocks near Monument Brook, in eastern Maine near Poplar Mountain (D. Hoy, pers. commun., 2001).

Recent detailed mapping (Fyffe, 1999) and geochemical analyses (Fyffe, 2001) have greatly improved the understanding of the local volcanic succession in the Eel River area. However, a description of the complete stratigraphic section of the Meductic Group is lacking because of the discontinuous nature of outcrop in the area. For this study, a discontinuous section of rocks along the Benton road was examined (Fig. 3), augmented by logging of nearby drillholes to elucidate stratigraphic relationships between the various lithotypes in the Meductic Group. Clarification of vertical and lateral stratigraphic relationships between formations of the Meductic Group may help to identify possible exploration targets by better defining the horizon containing the sulfide clasts.

Geological Setting

The northern Appalachians can be divided into four tectonostratigraphic zones from south to north: the Avalon, Gander, Dunnage, and Humber zones (Williams, 1979). The Gander zone is thought to represent a Lower Paleozoic west-facing passive margin deposited on the Avalonian platform, whereas the Dunnage zone represents remnants of oceanic crust, arcs, and back-arc basins. In New Brunswick, the Gander and Dunnage zones are exposed principally in the Miramichi terrane (Fig. 1; Fyffe and Swinden, 1992; van Staal, 1994; van Staal and Fyffe, 1995a,b).

The Eel River area is situated at the southwestern extremity of the Miramichi terrane (Fig. 1). The Cambrian to Ordovician sedimentary and volcanic rocks of the southwestern Miramichi terrane are separated from Late Ordovician to Late Silurian deep-water argillaceous carbonates and siliciclastic turbidites of the Matapedia basin to the north by the Woodstock fault (Bourque et al., 1995), and from Siluro-Devonian shallow marine limestone, conglomerate, and volcanic rocks of the Canterbury basin to the south by the Meductic fault (O'Brien, 1977; Fyffe, 2001). In the Millville area, Siluro-Devonian volcanic and sedimentary rocks of the Tobique Group divide the Miramichi Highlands into the southwestern and northeastern sections. The Bathurst Mining Camp at the northeastern terminus of the Miramichi Highlands, contains over 90 massive sulfide deposits and occurrences (Goodfellow and McCutcheon, 2003), which are hosted by a bimodal volcanic sequence in contrast to the unimodal sequence of the Eel River area.

The oldest rocks in the Eel River area consist of a continentally derived Cambrian to Early Ordovician turbidite sequence of the Woodstock Group (Fyffe et al., 1983; Pickerill and Fyffe, 1999). This Gander-like sequence is conformably overlain by mainly volcanic rocks of the Ordovician Meductic Group (Fyffe, 2001), which has been interpreted as forming in an island-arc setting over a southeast-facing subducting slab. Rifting of the arc started at 475 Ma, and subsequent opening of a back-arc basin resulted in the northwestern migration of active subduction (van Staal, 1987; Dostal, 1989; van Staal and Fyffe, 1995b). The sequence was subjected to considerably less ductile deformation and has incurred a lower grade of metamorphism than correlative rocks in the northeastern part of the Miramichi Terrane. Fyffe (2001) presented a comprehensive review of the stratigraphy in the Eel River area, and the following descriptions are summarized largely from this work.

Woodstock Group

The Woodstock Group has been divided into quartz wacke and shale of the Baskahegan Lake Formation, and mudstone and shale of the conformably overlying Bright Eye Brook Formation (Fig. 1; van Staal and Fyffe, 1995a,b; Pickerill and Fyffe, 1999). Rocks of the Woodstock Group are distinguished from those of the Miramichi Group in the northeastern part of the Miramichi Highlands by differences in lithology and contrasting geochemistry (Fyffe and Pickerill, 1993; Fyffe, 1994; Hennessy and Mossman, 1996; Fyffe, 2001).

Baskahegan Lake Formation

The Baskahegan Lake Formation is the stratigraphically lowest unit of the Woodstock Group (Fig. 1). Fossil occurrences in the Eel River area and in Maine have constrained the age of this formation to between Early Cambrian and Early Ordovician (Neuman, 1984; Pickerill and Fyffe, 1999). The formation is composed of medium- to thick-bedded quartzite, thin- to medium-bedded quartz wacke, silty shale, and lesser red sandstone and shale (Fyffe, 2001). Quartz wacke beds are typically graded, and display

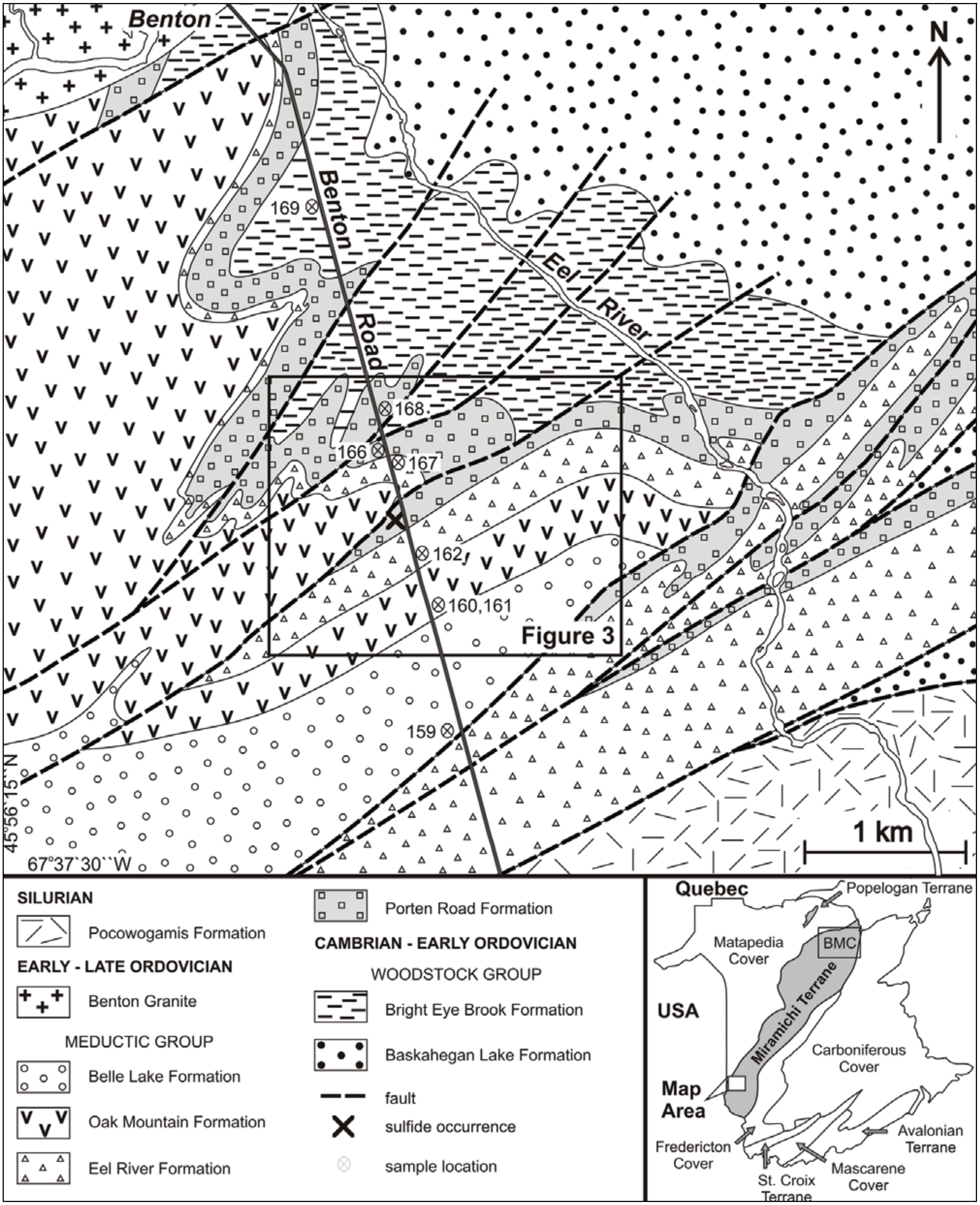

Fig. 1. Regional geological map of the Eel River area, west-central New Brunswick (modified from Fyffe, 1999), showing location of samples submitted for whole-rock analysis. Inset map of New Brunswick shows tectonostratigraphic subdivisions and location of the Bathurst Mining Camp (BMC) after Fyffe and Fricker (1987).

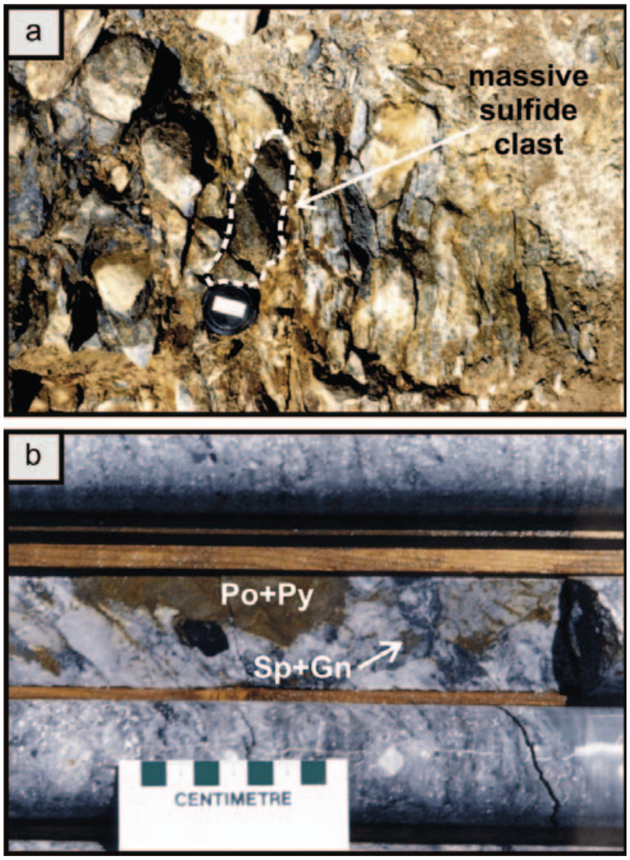

Fig. 2. ***a.*** Large sulfide clast uncovered in road cut along the Benton Road in the Eel River area. The clast (outlined in white) is mainly composed of pyrrhotite and pyrite, and is hosted by polylithic fragmental rocks (debris flows) of the Porten Road Formation; lens cap for scale. ***b.*** Similar sulfide fragments (pyrrhotite + pyrite) occur in DDH BB 95-10, which intersects debris flows from the Porten Road Formation. The blocky sulfide clast is accompanied by smaller fragments of black rhyolite and sphalerite, and is surrounded by fragments ranging from dacite to rhyolite in composition.

sedimentary structures such as load casts, flame structures, and ripple marks. Sandstone beds near the top of the Baskahegan Lake Formation decrease in thickness upwards, and form a gradational contact with the overlying Bright Eye Brook Formation (Fyffe, 2001).

Bright Eye Brook Formation

The Bright Eye Brook Formation is characterized by dark gray to black laminated silty mudstone, and highly carbonaceous and pyritiferous black shale (Fyffe, 2001). Graptolites found in black shale range from Late Tremadocian (Bailey, 1901; Fyffe et al., 1983) to Early Arenigian in age (Pickerill and Fyffe, 1999; Fyffe, 2001). This formation is coeval with the Patrick Brook Formation in the upper part of the Miramichi Group in the Bathurst Mining Camp (Goodfellow and McCutcheon, 2003). Deposition of black shale of the Bright Eye Brook Formation reflects anoxic marine conditions prior to the onset of volcanism associated with the overlying Meductic Group (Fyffe and Pickerill, 1993; Hennessy and Mossman, 1996). Similarly, in the Bathurst Mining Camp, carbonaceous shales occur in the Patrick Brook Formation underlying the volcanosedimentary sequence of the Bathurst Supergroup (Fyffe, 1994; van Staal and Fyffe, 1995a,b; Lentz et al., 1996).

Meductic Group

The Meductic Group consists of the following four formations in ascending order: Porten Road, Eel River, Oak Mountain, and Belle Lake formations (Fig. 1). The Porten Road and Eel River formations consist dominantly of felsic and intermediate volcanic rocks, the overlying Oak Mountain Formation is largely composed of mafic volcanic rocks, and the uppermost Belle Lake Formation consists of feldspathic wacke and shale (Fyffe, 2001). Stratiform massive sulfides and sulfide clasts occur within felsic volcanic and sedimentary rocks of the Porten Road Formation.

Porten Road Formation

The Porten Road Formation, the basal unit of the Meductic Group, includes massive to brecciated andesite, dacite, and rhyolite, sedimentary rocks, and lesser basalt. At the conformable lower contact with the Woodstock Group, black shale and mudstone of the Bright Eye Brook Formation grade upward into the Porten Road Formation (Fyffe, 2001).

Eel River Formation

The Eel River Formation comprises massive to brecciated andesite, bedded volcaniclastic rocks, massive basalt, and lesser ferromanganiferous mudstone and laminated maroon iron formation (Fyffe, 2001). The contact with the underlying Porten Road Formation is defined as the base of a medium-gray volcaniclastic sandstone containing plagioclase clasts and rare fragments of porphyritic rhyolite, as seen along the Porten road (Fyffe, 2001).

Oak Mountain Formation

Mafic volcanic rocks of the Oak Mountain Formation conformably overlie fragment-rich andesite breccia of the Eel River Formation. The Oak Mountain Formation consists of dark green, fine-grained, amygdaloidal porphyritic basalt, and minor pillow basalt, basaltic breccias, and fine-grained, bedded hyaloclastic rocks. Tops from pillow structures west of the Benton road indicate that the Oak Mountain Formation overlies the Eel River Formation. Red laminated chert and maroon to light green mudstone occur at the top of the Oak Mountain Formation (Venugopal, 1979; Fyffe, 2001).

Belle Lake Formation

The Belle Lake Formation consists of a clastic turbiditic sequence of light gray, thin-bedded, feldspathic wacke interstratified with medium-gray to black shale (Venugopal, 1978). Graptolites in shale from the Belle Lake Formation

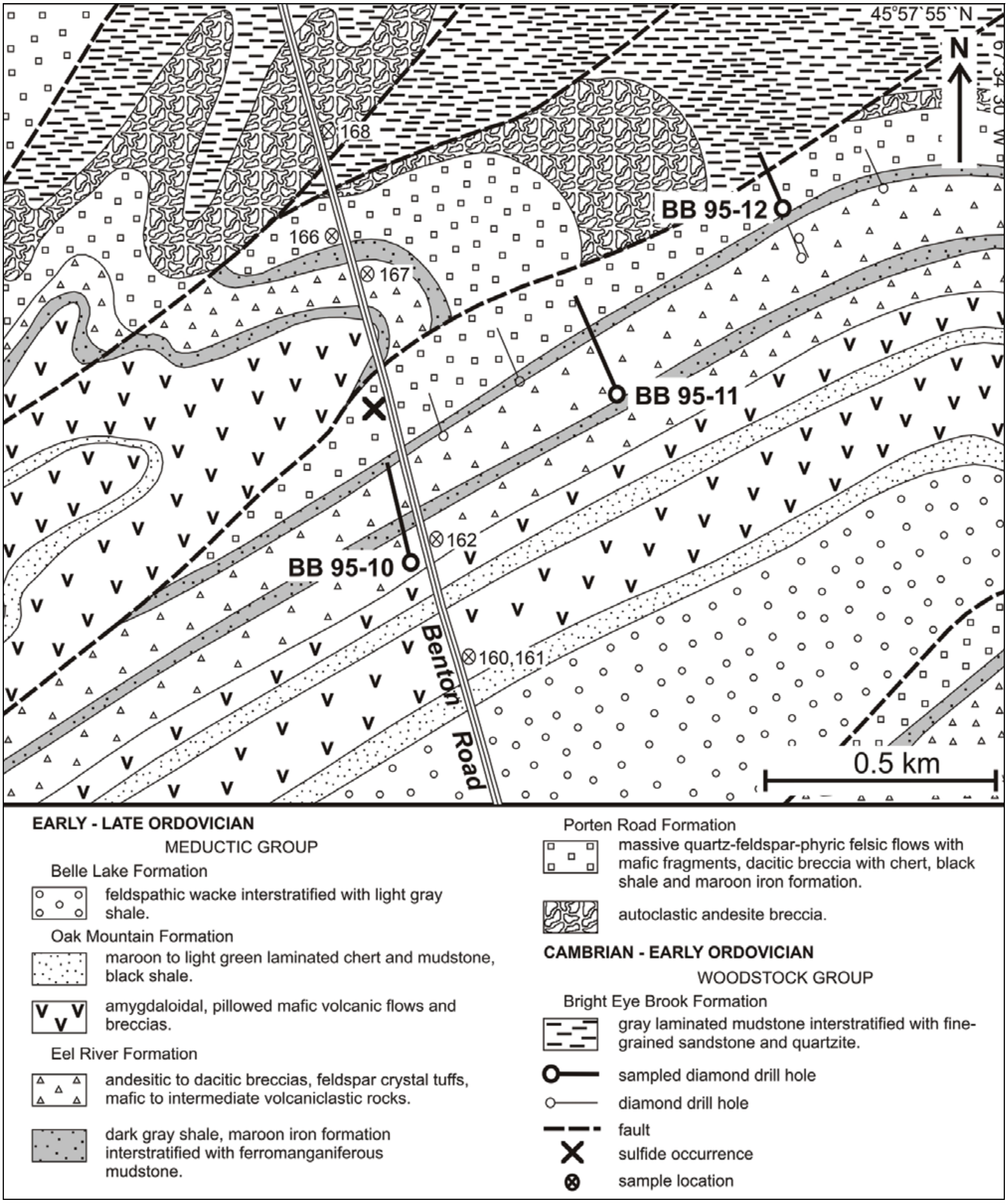

Fig. 3. Detailed geology of the Eel River area modified from Fyffe (1999), showing location of exploration drillholes examined and their contact relationships with previously mapped units. Core from labeled drillholes was examined for this study.

indicate an Early Caradocian age (Fyffe et al., 1983). At the base of the Belle Lake Formation, wacke and shale conformably overlie red chert and mudstone of the Oak Mountain Formation (Fyffe, 2001).

Drillhole Stratigraphy

Three diamond-drill holes (DDHs BB 95-10, -11, -12) from the Eel River area (Fig. 3) were examined in detail to elucidate stratigraphic relationships between various lithotypes of the Meductic Group, and to determine intra-formational variations along strike. The three drillholes provide a good stratigraphic cross section through the Eel River and Porten Road formations of the Meductic Group (Fig. 3). Information derived from detailed logging of these holes augments information obtained by Fyffe (2001) from surface exposures of the Eel River and Porten Road formations. Rocks from the Bright Eye Brook, Oak Mountain, and Belle Lake formations were not encountered in drillholes; however, samples of these formations were collected from outcrops along the Benton road.

Porten Road Formation

Drillhole BB 95-12 (Fig. 4) transects a thick sequence of volcanic rocks interlayered with lesser sedimentary rocks of the Porten Road Formation. The oldest rocks consist of a plagioclase-phyric hyaloclastite (Figs. 5a,b) with an intermediate composition. Fragments are gray-green in color and contain approximately 10% plagioclase crystals, 1 to 2 mm in width. Fragments range in size from 1 to 10 cm, have

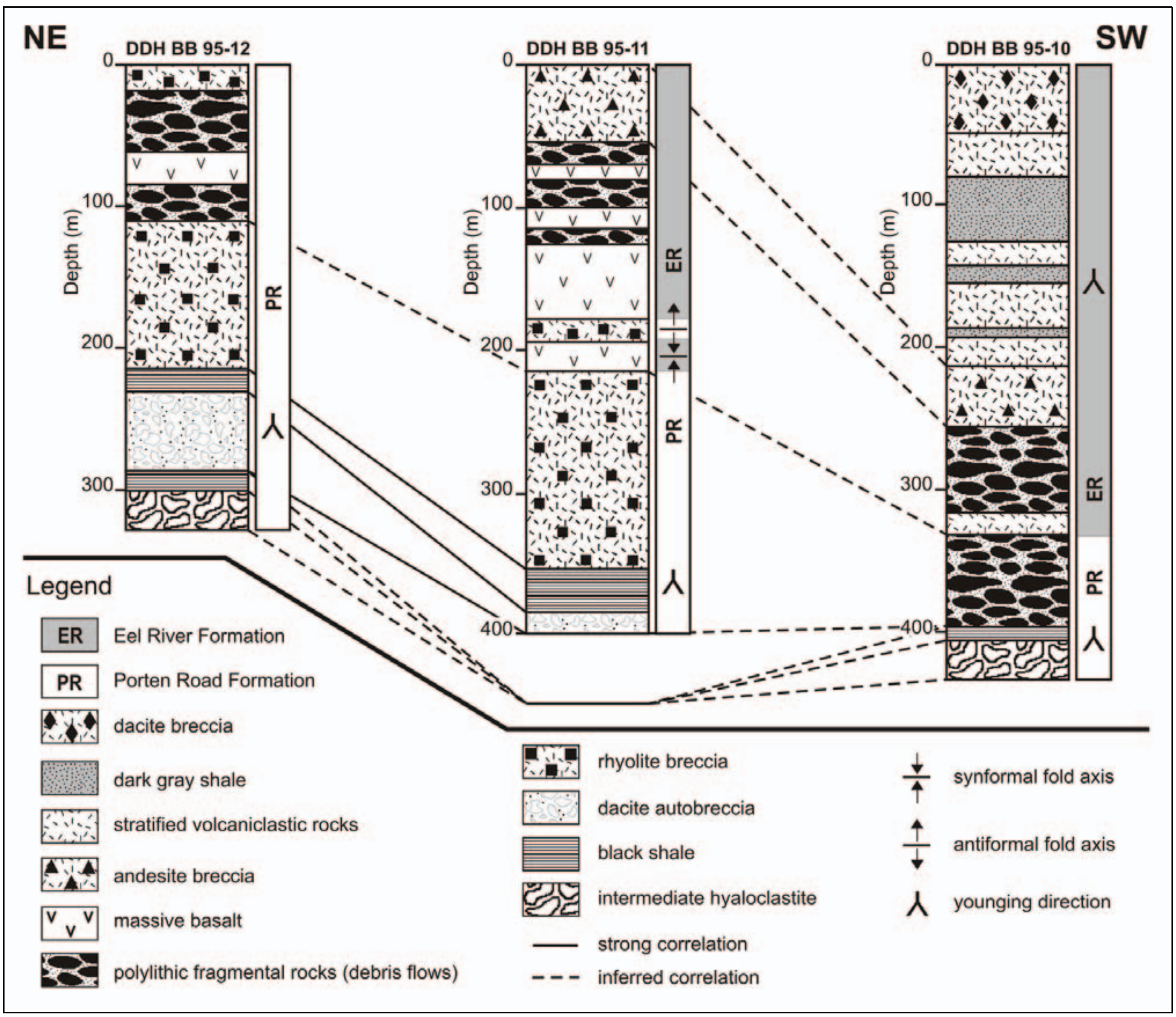

Fig. 4. Drillhole stratigraphic correlations in the Porten Road and Eel River formations (DDHs BB 95-10, -11, -12). Lateral variations exhibit a proximal to distal transition from DDH 95-12 in the northeast to DDH 95-10 in the southwest (see Fig. 3).

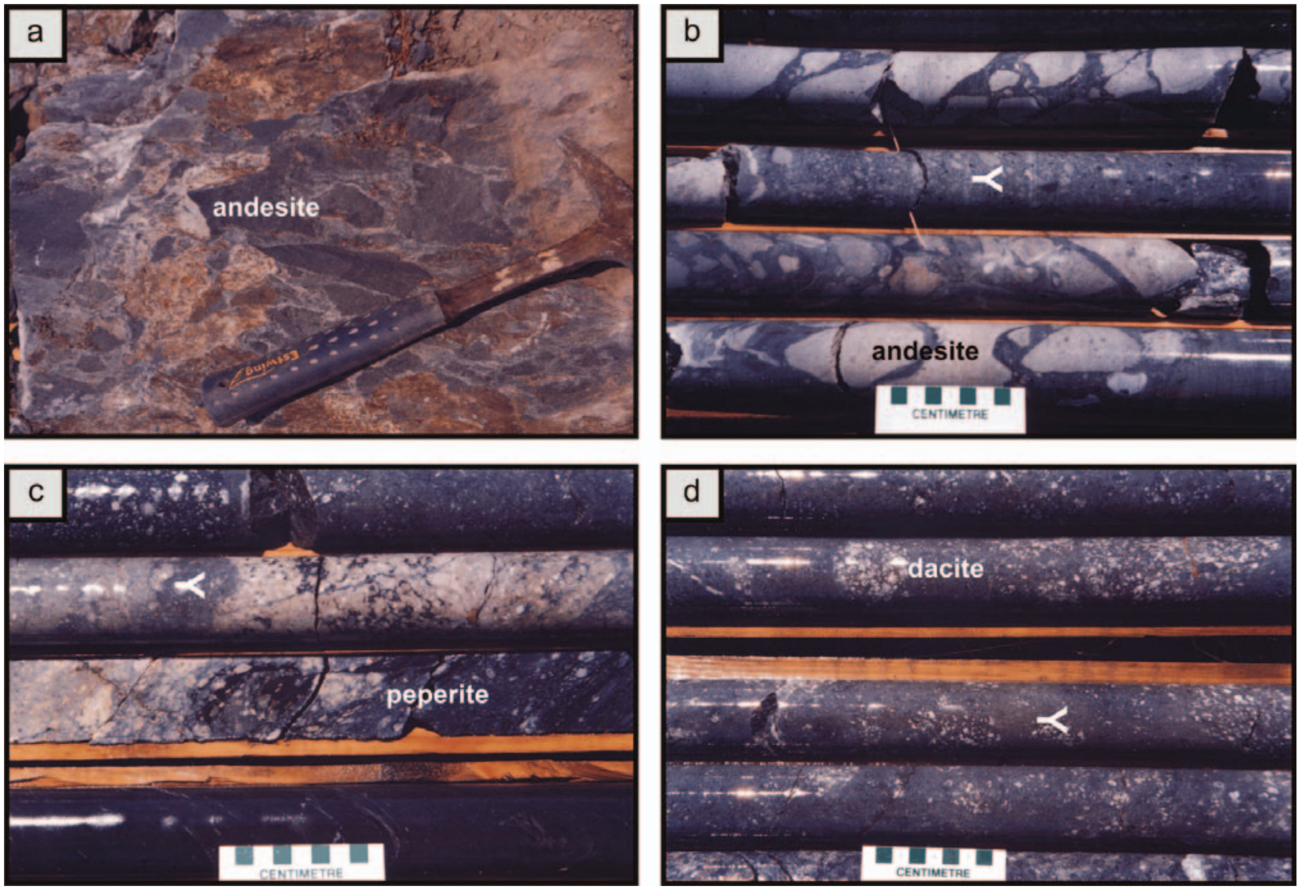

Fig. 5. Surface exposure and drill core photographs illustrating submarine volcanic breccias and flows from the Porten Road Formation, Meductic Group. ***a.*** Hyaloclastite in a road cut of the Benton Road (sample 168), consisting of angular fragments of porphyritic andesite in a matrix of plagioclase microlites (Fyffe, 2001). ***b.*** Intermediate-composition hyaloclastite from the base of the Porten Road Formation intersected in DDH BB 95-12 (309–314 m). The jigsaw fit of the fragments indicates quenching with seawater during eruption on the seafloor. ***c.*** Peperitic breccia consisting of cream-colored globules of rhyolite suspended in black shale of the lower Porten Road Formation (DDH BB 95-12; 287 m). ***d.*** Dacite autobreccia (DDH BB 95-12; 277–280 m) containing fragments of dacite in a felsic groundmass of similar composition.

sharp fragment boundaries, and form a jigsaw fit with other fragments, indicating in situ quenching of the lava during eruption on the seafloor (see Cas, 1992). This hyaloclastite is also encountered at the base of DDH BB 95-10 (Fig. 4) and in outcrops on the Benton Road (Fig. 5a), where blocks of the underlying Bright Eye Brook shale have been incorporated in these hyaloclastites during eruption (Fyffe, 2001).

The intermediate hyaloclastite is overlain by a 14 m-thick unit of black shale and lesser wacke. The black shale contains wisps, veinlets, and small pods of pyrrhotite and pyrite that are closely associated with late calcite veinlets. This black shale unit is also encountered in DDH BB 95-10 (Fig. 4), where the shale is only 7 m thick. This unit is similar to black shale in the underlying Bright Eye Brook Formation, and indicates that anoxic conditions prevailed for a considerable period of time. At the top of the shale unit in drillhole BB 95-12, a 30 cm section of peperitic breccia (Fig. 5c) composed of small globules (<5 mm) and larger lapilli-size fragments of cream-colored felsic volcanic rock enclosed within black shale, indicates eruption of a felsic lava into wet unconsolidated sediments.

The black shale and peperitic breccia are overlain by a 51 m-thick sequence of dacite autobreccia (Fig. 4). The autobreccia consists of large fragments of plagioclase-phyric dacite in an aphanitic to phaneritic felsic groundmass (Fig. 5d). The fragments are up to 10 cm wide, and contain 15% euhedral plagioclase phenocrysts that range in width from 1 to 5 mm. Fragment boundaries are barely discernable, which is likely due to in situ fragmentation during flow of a solidifying lava. Furthermore, Fyffe (2001) has documented flow-aligned microlites in the groundmass of similar breccias along the Benton Road. Drillhole BB 95-11 ends in this autobreccia, and does not intersect the underlying black shale and intermediate hyaloclastite (Fig. 4).

The dacite autobreccia is overlain by 16 m of black shale compositionally similar to the lower shale unit, but containing more sulfides. This upper black shale unit is also encountered in drillhole BB 95-11 where it reaches a thickness of 30 m, but is not intersected by DDH BB 95-10 (Fig. 4). The lower and upper black shale units constitute distinct horizons in the Porten Road Formation and are readily recognizable in drill core. A polylithic fragmental unit (5 m thick) at the base of the upper black shale is composed of blocks of dacite and mudstone likely representing slumps derived from the underlying dacite autobreccia and black shale.

The upper black shale unit in DDHs BB 95-11 and 95-12 is overlain by a thick sequence (up to 140 m) of rhyolite breccia (Fig. 4), containing quartz- and feldspar-rich volcaniclastic sections, blocks of massive rhyolite, and lesser sedimentary clasts. Rhyolite fragments are quartz-phyric with phenocrysts ranging from 2 to 3 mm in length. The volcaniclastic sections contain 7% to 10% subhedral plagioclase phenocrysts (1–2 mm long) and may represent reworked felsic breccia. The quartz content is much more variable, averaging 15% overall with equant grains ranging from 1 to 3 mm. Some quartz phenocrysts in rhyolite fragments and in volcaniclastic sections are surrounded by an oval-shaped siliceous envelope 3 to 5 mm in length.

The rhyolite breccia in DDH BB 95-12 is overlain by a sequence of variably altered polylithic fragmental rocks (Fig. 4) containing lapilli and blocks of basalt, dacite, and rhyolite in a volcaniclastic groundmass (Fig. 6a). These fragmental rocks surround a 23 m-thick unit of plagioclase-phyric, massive to fragmental basalt that locally contains carbonate-filled amygdules up to 1 cm across. The eruption of this basalt likely resulted in slumping on the flanks of the volcanic edifice, and disruption of the underlying rhyolite breccia.

To the southwest, in drillhole BB 95-10, the intermediate hyaloclastite and black shale units at the base of the Porten Road Formation are overlain by polylithic fragmental rocks (Fig. 4). These fragmental rocks are dominantly felsic in composition, but also contain fragments of andesite, basalt, mudstone, and sulfide. A blocky, elongate clast of massive sulfide, 7 cm in length, occurs in this attenuated section and is composed of pyrrhotite and pyrite (Fig. 2b). This and smaller sulfide clasts are accompanied by fragments of black and cream-colored rhyolite containing syndeformational veinlets of remobilized pyrite and pyrrhotite. Ductile behavior of sulfides after transport has resulted in syndeformational veining of some felsic fragments, which may be misinterpreted as stockwork mineralization. Smaller blebs and wisps of pyrrhotite, pyrite, sphalerite, and galena also occur throughout the section. The blocky nature of the larger clast indicates that sulfides were consolidated and underwent brittle deformation (McClay and Ellis, 1983) during transport in debris flows.

Fyffe (2001) describes outcrops of this fragmental unit along the Benton Road as having formed through explosive pyroclastic volcanism and syn-volcanic flow along the flanks of a felsic dome. This is substantiated by the intersection of a 68 m-thick unit of quartz- and feldspar-rich rhyolite porphyry in drillhole BB 94-7, 250 m to the east of DDH BB 95-12 (Fig. 3). The porphyry contains 5% to 20% euhedral feldspar phenocrysts, 2 to 8 mm in size (Williamson, 1996), and is locally autobrecciated. It is overlain by black shale, which is in turn overlain by stratiform massive sulfides. The occurrence of sulfide fragments in polylithic fragmental rocks, intersected in drillhole BB 95-10, and in the road cut along the Benton Road, indicates a probable transport of these rocks in debris flows from a source area to the northeast (Fig. 3).

Eel River Formation

In drillhole BB 95-10, the lower contact of the Eel River Formation is defined as the base of an intermediate volcaniclastic rock interbedded with dark gray shale, which overlies debris flows of the Porten Road Formation (Fig. 4). This 16 m-thick volcaniclastic unit is plagioclase-phyric, and grades from a coarse-grained base (plagioclase; 1–2 mm) to a fine-grained top.

In drillhole BB 95-11, the lowermost rocks of the Eel River Formation consist of plagioclase-phyric basalt, which forms a sharp boundary (Fig. 6b) with an underlying unit of felsic breccia from the Porten Road Formation. A 100 m interval of tight folding is characterized by the repetition of felsic and mafic volcanic rocks of the Porten Road and Eel River formations, respectively (Fig. 4). Lithogeochemical data (see below) indicate that this basalt is distinct from basalt of the Porten Road Formation; in other respects, they are indistinguishable and probably genetically related.

Volcaniclastic rocks in DDH BB 95-10 are overlain by polylithic fragmental rocks composed of rounded lapilli and blocks of rhyolite, dacite, andesite, basalt, and mudstone in a dominantly volcaniclastic groundmass; the fragments are irregularly shaped and variably altered. These polylithic fragmental rocks are interlayered with dark gray mudstone and wacke, and were likely deposited from debris flows. Similar debris flows also disrupt units of massive basalt in DDH BB 95-11 (Fig. 4).

Debris flows in drillhole BB 95-10 are overlain by a 42 m-thick section of andesite breccia, which also occurs along strike to the northeast in DDH BB 95-11 (Fig. 4). The breccia consists of massive andesite fragments with lesser mudstone and local fragments of dacite in a fine-grained quartz- and feldspar-rich volcaniclastic groundmass. Fragment abundance is variable throughout the unit with some volcaniclastic sections having no fragments.

The andesite breccia in drillhole BB 95-10 is overlain by a uniform, 164 m-thick section of plagioclase-rich volcaniclastic rocks interbedded with generally fine-grained sedimentary rocks (Fig. 4). Plagioclase phenoclasts range from less than 1 to 2 mm in size and vary in abundance. Individual layers are graded with a coarse base progressing to a fine-grained laminated top intimately mixed with dark gray shale (Fig. 6c,d). The graded sequences are interbedded with dark gray shale and wacke (beds are typically less than 13 m thick) indicating somewhat quiescent conditions in a distal environment. Slump folds identified in drill core and in

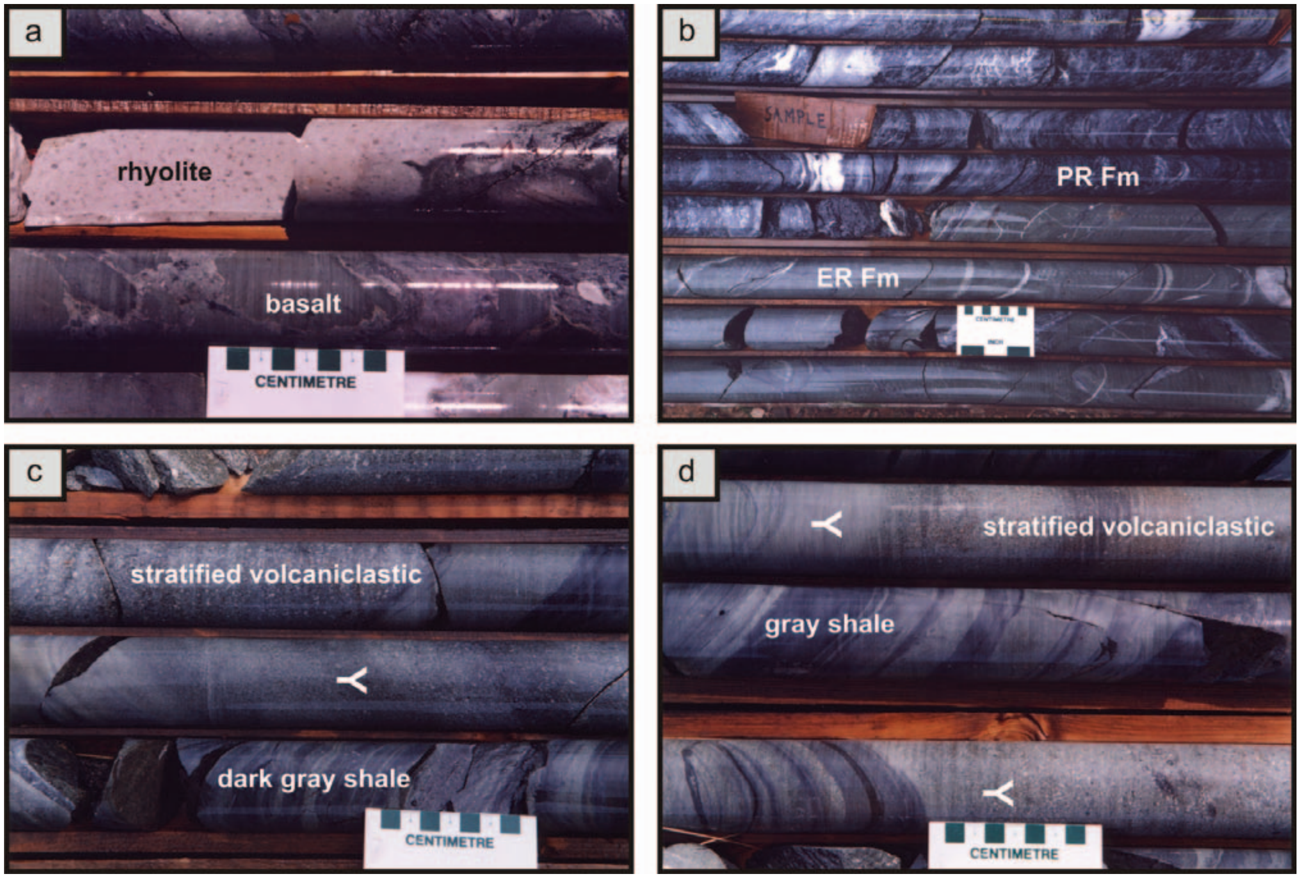

Fig. 6. Drill core photographs of volcanic and sedimentary rocks from the Porten Road and Eel River formations, Meductic Group. ***a.*** Polylithic fragmental rocks (Porten Road Formation) consisting dominantly of basalt fragments with lesser variably altered plagioclase-phyric rhyolite in a feldspar-rich groundmass (DDH BB 95-12; 33–64 m). ***b.*** Drill core displaying the contact between mafic volcanic rocks of the Eel River Formation (lower section) and reworked felsic breccias from the Porten Road Formation (DDH BB 95-11; 189–199 m). ***c.*** A sequence of plagioclase-rich volcaniclastic rocks interbedded with dark gray mudstone, Eel River Formation. Volcaniclastic rocks fine upwards throughout the section (DDH BB 95-10; 168–171 m). ***d.*** A fining-upward sequence of mafic to intermediate volcaniclastic rocks interbedded with dark gray mudstone (DDH BB 95-10), Eel River Formation.

exposed volcaniclastic rocks west of Porten Settlement (Fyffe, 2001) indicate deposition on a slope. The bedded sequences are locally interrupted by polylithic fragmental rocks similar to debris flows at the base of the Eel River Formation. Dark gray shale interbedded with the volcaniclastic rocks forms several thick accumulations (attaining 46 m in thickness), indicating significant breaks in volcanic activity. The dark gray shale contains numerous bands of wacke, and thin layers of plagioclase-rich volcaniclastic material containing minor pyrrhotite. The dark gray shale is also laminated with pyrrhotite, pyrite, and calcite along partings.

Stratified volcaniclastic rocks in drillhole BB 95-10 are overlain by a 48 m-thick unit of massive to brecciated dacite (Fig. 4). This variably altered breccia contains plagioclase-phyric sections and lesser sedimentary clasts indicating minor reworking. Lithogeochemical data (see below) indicate that this dacite breccia and the felsic fragments in debris flows towards the base of the Eel River Formation are geochemically distinct from Porten Road felsic volcanic rocks.

Sampling and Analytical Methodology

Representative samples of volcanic and sedimentary rocks were collected from the three drillholes (DDH BB 95-10, -11, -12) intersecting rocks belonging to the Porten Road and Eel River formations in the vicinity of sulfide breccias outcropping along the Benton Road. Samples consisted of a 0.3 to 0.6 m section of halved drill core, as well as a 15 cm slab for a polished section. In the case of polylithic fragmental rocks, large fragments of the most dominant lithotype were carefully cut to avoid alteration rims and incorporation of the matrix. For fine-grained breccias and fragmental rocks, several samples were collected over a 3 to 5 m interval and combined, to ensure uniform sampling of the unit. Surface exposures along the Benton road were also sampled to correlate geochemical data from drill core to previously mapped units (Fyffe, 2001), and also to obtain data for the Bright Eye Brook, Oak Mountain, and Belle Lake formations, which were not intersected in drillholes. Samples were crushed in a steel jaw crusher and a portion was pulverized in a soft iron swingmill. Samples and a rhyolite standard (NB-94-RHY; Lentz, 1995) were submitted for major and trace element analysis by X-ray fluorescence (XRF) pressed powder procedures (Longerich, 1995) at Memorial University in St. John's, Newfoundland. Geochemical results are listed in Table 1. High analytical accuracy was achieved for SiO_2, TiO_2, $Fe_2O_3^T$, MnO, Na_2O, K_2O, Ga, Rb, Sr, Y, and Ba with error values less than 5% (relative). Al_2O_3, Sc, V, Zr, and Nb analyses display less than 15% calculated error, but exhibit good reproducibility, with a relative standard deviation ranging from 0.006% to 0.25%. Some major elements, such as MgO, CaO, and P_2O_5, and several trace elements (Cr, Zn, and Th) exhibit higher analytical errors.

Lithogeochemistry

Volcanic rocks in the Eel River area represent a complete calc-alkaline suite ranging from subalkaline basalt to rhyolite (Fig. 7). These rocks have been hydrothermally altered to varying degrees affecting their Si, Na, and K contents, a result of low- to high-temperature metasomatism by heated seawater (Galley, 1995; Fig. 8). These rocks form distinct groups based on their SiO_2 contents, although simple classification based on SiO_2 contents alone is invalidated due to the mobility of silica during alteration and metamorphism. A more effective geochemical means for discriminating rocks is through the use of Zr, TiO_2, Nb, and Y (Fig. 9; see Winchester and Floyd, 1977). These elements are generally immobile during alteration and metamorphism, and are assumed to reflect primary compositional variations of a fractionating magma that is responsible for the diverse lithotypes found throughout the Eel River area.

Overall, the Eel River Formation exhibits a mafic to intermediate affinity compared to the Porten Road Formation, which is dominantly felsic in composition. However, both formations contain subalkaline basalt, andesite, and dacite lithotypes; rhyolite is exclusive to the Porten Road Formation. Felsic and intermediate rocks belonging to the Porten Road Formation may be distinguished from those of the Eel River Formation through the use of Zr/TiO_2 and Nb/Y ratios (Fig. 9).

Felsic Units

Rhyolite in the Porten Road Formation occurs as massive flows, and as fragments in reworked breccias and debris flows. Rhyolites are geochemically distinguished from dacitic and andesitic rocks by their higher Zr/TiO_2 ratios, which average 0.198 and range from 0.139 to 0.286 (Fig. 9). Fyffe (2001) has further subdivided rhyolites into a light rare earth element (LREE) enriched group with MgO contents ranging between 1.7 and 4.1 wt.%, and a heavy rare earth

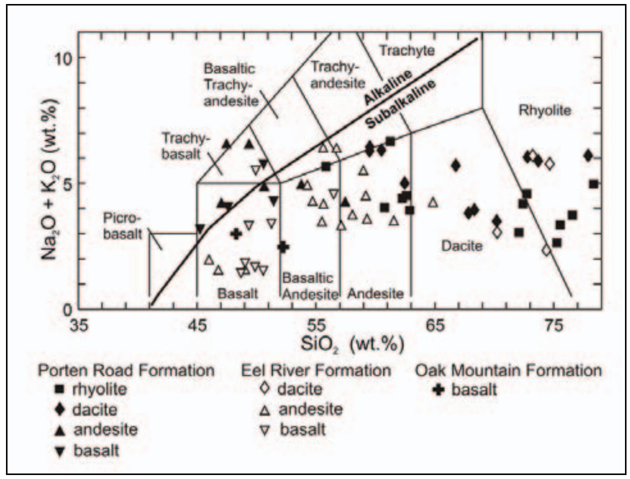

Fig. 7. Total alkali–silica diagram after Le Bas et al. (1986) displaying the range of compositions for volcanic rocks from the Meductic Group. Sample lithologies defined by immobile trace element ratios and field descriptions. Alkaline/subalkaline boundary after Irvine and Baragar (1971).

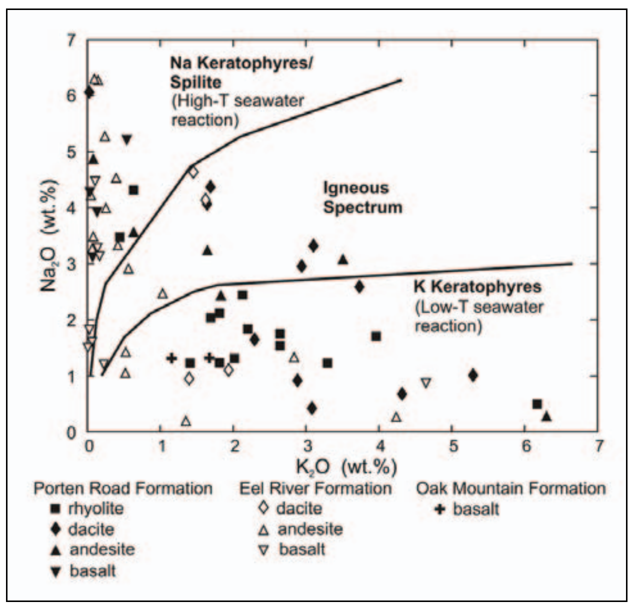

Fig. 8. Igneous spectrum diagram derived from Hughes (1972) displaying the effects of seawater alteration on volcanic rocks from the Eel River area.

element (HREE) enriched group with MgO ranging from 0.9 to 2.0 wt.%. The SiO_2 content of the rhyolites is highly variable, ranging from 54.1 to 77.1 wt.%, and averaging 68.5 wt.% SiO_2. The high variability of silica is likely a result of hydrothermal alteration, which has also affected Na_2O (0.48–4.18 wt.%), K_2O (0.42–5.99 wt.%), CaO (0.45–15.27 wt.%), and MgO (0.23–7.85 wt.%) contents (Table 1).

Dacitic rocks of the Porten Road Formation occur as brecciated lava flows and as fragments in polylithic fragmental rocks. Porten Road dacite may be distinguished

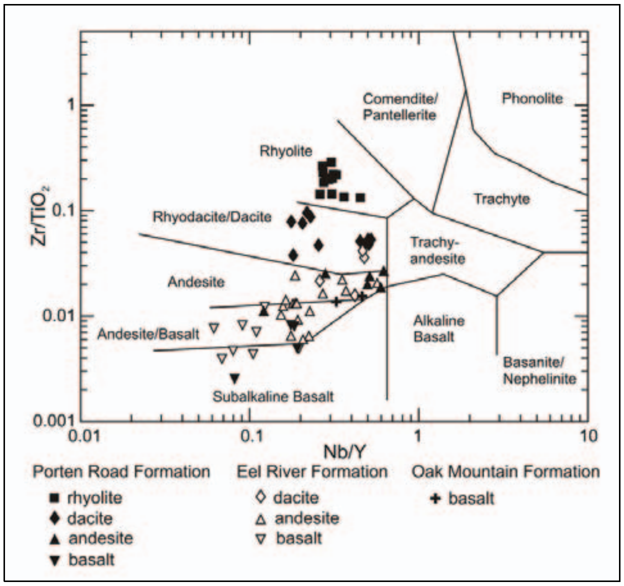

Fig. 9. Zr/TiO_2 vs. Nb/Y compositional discrimination plots for volcanic rocks (after Winchester and Floyd, 1977) of the Meductic Group.

from rhyolite by its higher plagioclase content and lower Zr/TiO_2, averaging 0.063 (0.038–0.099; Fig. 9). The SiO_2 content of Porten Road dacites ranges from 55.4 to 75.0 wt.%, with an average of 65.1 wt.% SiO_2. In addition to silica, alteration has also led to variable contents of $Fe_2O_3^T$ (1.55–7.41 wt.%), MgO (1.00–5.85 wt.%), Na_2O, K_2O, and CaO (Table 1). Dacite from the Eel River Formation occurs as fragments in hyaloclastite and polylithic fragmental rocks, and can be distinguished from felsic volcanic rocks of the Porten Road Formation by its lower Zr/TiO_2, which averages 0.030 (0.016–0.043; Fig. 9). SiO_2 contents of Eel River dacites are higher, averaging 71.0 wt.% (69.4–73.6 wt.%). The average MnO content of the dacite is 0.18 wt.%, but ranges from 0.07 to 0.38 wt.%, possibly due to contributions from intercalated mafic material, which may have also affected Zr, TiO_2, Nb, and Y contents (Table 1).

Intermediate Units

This term is applied to volcaniclastic rocks, massive flows, and hyaloclastite that range in composition from basaltic andesite to andesite. Intermediate rocks are voluminous in the Eel River Formation, forming a thick sequence of stratified volcaniclastic rocks interlayered with light gray mudstone. Intermediate rocks also occur in brecciated flows and as fragments in polylithic fragmental rocks. The SiO_2 content of intermediate rocks from the Eel River Formation ranges from 41.9 to 61.2 wt.% SiO_2, overlapping with basalt and dacite compositions. However, Zr/TiO_2 ratios clearly show that these altered rocks have a basaltic andesite to andesite composition (Fig. 9). Zr/TiO_2 averages 0.014 (0.007–0.025), Nb/Y averages 0.24 (0.15–0.57), and Ba averages 247 ppm (28–880 ppm; Table 1).

Intermediate rocks of the Porten Road Formation occur in a hyaloclastite unit at the base of the Meductic Group, overlying sedimentary rocks of the Bright Eye Brook Formation (Woodstock Group). Nb/Y ratios of intermediate rocks from the Porten Road Formation average 0.44 (0.12–0.62), much higher than the Eel River Formation (Fig. 9). Furthermore, Zr/TiO_2 is higher for intermediate rocks from the Porten Road Formation, averaging 0.022 (0.012–0.028). The Ba content of intermediate rocks from the Porten Road Formation is also much higher than that from the Eel River Formation, with an average of 1993 ppm (45–5885 ppm; Table 1). The average SiO_2 content of these intermediate rocks is 47.7 wt.% (42.3–54.7 wt.%), indistinguishable from their counterparts in the Eel River Formation. Thorium was found to be, for the most part, below the detection limit in intermediate rocks throughout the Eel River area (Table 1).

Mafic Units

Near the top of the Porten Road Formation, mafic volcanic rocks occur as massive units and fragments in polylithic fragmental rocks. The SiO_2 content of the basalt averages 44.5 wt.% (41.6–47.4 wt.%), and $Fe_2O_3^T$ averages 13.5 wt.% (12.4–14.9 wt.%). Low average contents of TiO_2 (0.41 wt.%), P_2O_5 (0.07 wt.%), Zr (25 ppm), and Nb (1.8 ppm) reflect their subalkaline character. The average V content is 353 ppm, with a range of 293 to 469 ppm (Table 1).

Basalt abundance increases in the Eel River Formation, occurring as massive flows and in polylithic fragmental rocks. The average SiO_2 content of Eel River basalt is 47.8 wt.% (45.5–52.5 wt.%), whereas $Fe_2O_3^T$ averages 13.3 wt.% (8.5–17.6 wt.%), and Al_2O_3 averages 13.4 wt.% (11.2–20.5 wt.%). These rocks are also subalkaline, reflected in their low average contents of TiO_2 (0.33 wt.%), Zr (22 ppm), and Nb (0.9 ppm). The Nb/Y ratio is slightly lower in Eel River basalt (0.10) than in the Porten Road Formation (0.16; Fig. 9). Basalt from the Eel River Formation also has lower P_2O_5 contents averaging 0.03 wt.% (Table 1).

Massive to brecciated basalt from the Oak Mountain Formation is the most voluminous volcanic lithotype in the Meductic Group. In two samples collected along the Benton Road (Fig. 1; samples 160 and 161), SiO_2 ranges from 44.6 to 50.6 wt.%, Al_2O_3 ranges from 13.6 to 13.8 wt.%, and $Fe_2O_3^T$ from 13.5 to 13.6 wt.%, similar to values for Porten Road and Eel River basalts (Table 1). However, Oak Mountain basalt has higher contents of TiO_2 (0.66–0.68 wt.%), P_2O_5 (0.16–0.33 wt.%), Zr (97–108 ppm), and Nb (8.1–8.8 ppm; Table 1). These calc-alkaline characteristics are markedly different from basalt of the underlying Porten Road and Eel River formations (Fig. 10), which are less alkaline and plot in the MnO-rich sector of the calc-alkaline field (Fig. 11), although some compositional overlap may occur between the Eel River and Oak Mountain basalts (Fyffe, 2001).

Table 1. Major and Trace Element Compositions of Volcanic and Sedimentary Rock from Drill Core and Surface Samples in the Eel River Area, West-central New Brunswick

Sample	Drillhole	Lithology	Fm.	Depth (m)	SiO_2 (wt.%)	TiO_2 (wt.%)	Al_2O_3 (wt.%)	$Fe_2O_3^T$ (wt.%)	MnO (wt.%)	MgO (wt.%)	CaO (wt.%)	Na_2O (wt.%)	K_2O (wt.%)	P_2O_5 (wt.%)	Total (wt.%)
1	95-10	dacite	ER	11.6	71.52	0.37	12.55	3.37	0.07	1.52	4.26	0.92	1.34	0.07	96.16
3	95-10	dacite	ER	38.2	69.46	0.39	14.24	4.34	0.09	2.76	4.19	1.09	1.92	0.09	98.84
6	95-10	andesite	ER	55.1	51.92	0.41	15.03	9.89	0.20	7.30	5.26	2.72	0.53	0.10	93.56
7	95-10	andesite	ER	63.6	58.14	0.34	14.23	7.76	0.23	5.66	4.41	2.32	0.98	0.06	94.48
10	95-10	gray mudstone	ER	80.8	63.06	0.66	15.55	8.55	0.18	3.22	1.95	1.29	3.42	0.04	98.26
14	95-10	andesite	ER	130.2	42.37	0.48	13.26	16.49	0.64	9.56	6.08	0.17	1.22	0.04	90.55
15	95-10	gray mudstone	ER	134.9	59.91	0.75	15.58	10.44	0.25	3.81	1.89	0.93	3.60	0.05	97.69
16	95-10	andesite	ER	138.2	51.82	0.37	15.53	10.65	0.57	4.83	5.23	1.24	2.64	0.06	93.17
17	95-10	gray mudstone	ER	147.7	60.12	0.78	16.24	10.05	0.26	2.98	1.01	0.99	3.88	0.03	96.72
18	95-10	gray mudstone	ER	153.2	56.61	0.71	15.58	10.82	0.33	3.42	3.41	1.16	3.34	0.11	96.10
20	95-10	andesite	ER	160.6	44.20	0.36	12.67	12.58	0.31	12.72	5.55	0.94	0.47	0.03	90.18
21	95-10	andesite	ER	172.4	41.86	0.41	13.73	12.80	0.39	13.40	6.40	1.29	0.48	0.03	91.01
24	95-10	gray mudstone	ER	190.2	59.54	0.73	14.99	9.04	0.17	4.01	2.31	2.06	2.72	0.27	96.16
26	95-10	andesite	ER	200.4	51.55	0.33	14.38	9.66	0.15	5.71	2.88	5.71	0.10	0.06	90.85
29	95-10	andesite	ER	227.7	61.16	0.34	13.00	7.02	0.16	4.11	4.20	3.76	0.24	0.06	94.32
30	95-10	andesite	ER	237.2	50.08	0.42	14.75	12.52	0.15	4.51	3.58	4.18	0.37	0.03	92.32
31	95-10	andesite	ER	245.7	54.72	0.38	14.12	9.70	0.20	4.73	3.61	4.89	0.22	0.06	92.77
32	95-10	gray mudstone	ER	266.2	57.11	0.74	16.93	12.62	0.59	2.85	1.25	0.65	3.21	0.05	96.26
37	95-10	gray mudstone	ER	290.1	63.05	0.86	17.24	8.50	0.19	3.78	1.32	1.35	2.92	0.04	99.46
39	95-10	gray mudstone	ER	299	57.46	0.93	19.72	9.20	0.26	3.12	1.48	0.59	4.44	0.21	97.62
40	95-10	gray mudstone	ER	307.7	55.06	0.94	20.14	10.84	0.32	2.66	1.33	0.28	4.71	0.06	96.57
42	95-10	andesite	ER	329	49.43	0.42	13.51	12.02	0.22	6.99	3.72	3.82	0.04	0.04	90.36
48	95-10	basalt	ER	370	52.49	0.21	12.49	7.92	0.16	10.13	4.84	4.16	0.10	0.04	92.86
50	95-10	dacite	PR	385	68.86	0.15	16.16	3.33	0.05	3.93	1.83	0.42	3.02	0.01	98.06
53	95-10	black shale	PR	403.7	70.67	0.70	15.51	4.63	0.06	3.34	1.43	1.04	2.86	0.23	104.10
55	95-10	andesite	PR	414.4	54.73	0.56	17.58	9.41	0.09	4.65	3.61	2.31	1.75	0.15	95.24
56	95-10	andesite	PR	415.6	46.62	0.62	19.34	10.19	0.08	4.14	5.93	2.97	1.52	0.13	91.99
57	95-10	gray mudstone	PR	420.3	66.32	0.75	17.27	4.64	0.04	3.67	1.76	1.69	2.99	0.16	100.65
58	95-11	andesite	ER	8.5	55.93	0.40	13.30	10.00	0.23	6.81	4.01	3.28	0.08	0.05	94.36
59	95-11	andesite	ER	23	56.45	0.41	14.59	9.91	0.22	6.94	4.31	3.23	0.41	0.06	97.23
62	95-11	andesite	ER	46.2	52.97	0.41	13.67	9.96	0.21	7.04	5.22	3.02	0.06	0.07	92.74
66	95-11	basalt	ER	76.3	45.54	0.67	14.21	16.21	0.33	6.33	5.67	2.91	0.15	0.08	92.25
67	95-11	dacite	ER	89	73.56	0.27	13.84	1.77	0.38	1.08	1.74	4.08	1.60	0.09	98.51
69	95-11	dacite	ER	97.1	69.43	0.22	13.41	3.07	0.19	1.56	0.99	4.41	1.38	0.05	94.79
72	95-11	basalt	ER	101.8	49.35	0.28	20.50	14.11	0.25	5.86	2.77	0.87	4.59	0.02	98.82
74	95-11	basalt	ER	109.1	45.45	0.24	11.70	14.42	0.23	13.94	5.72	1.13	0.21	0.01	93.24
75	95-11	basalt	ER	112.5	48.09	0.28	13.47	10.95	0.16	10.28	7.19	3.08	0.13	0.01	93.81
76	95-11	dacite	PR	117.1	70.39	0.13	14.76	2.63	0.04	1.82	0.97	4.22	1.64	0.02	96.71
78	95-11	basalt	ER	139.2	47.47	0.32	11.52	12.19	0.23	12.18	9.44	1.54	0.06	0.02	95.17
79	95-11	basalt	ER	164.2	46.07	0.30	11.24	12.26	0.28	10.87	10.90	1.73	0.03	0.03	93.92
81	95-11	dacite	PR	181.2	75.02	0.11	11.54	1.71	0.13	1.13	0.63	5.85	0.03	0.03	96.28
82	95-11	rhyolite	PR	189.3	62.82	0.10	21.83	2.94	0.09	7.09	0.74	2.11	1.81	0.01	99.90
83	95-11	basalt	ER	207.5	47.75	0.30	11.72	12.07	0.37	12.53	8.03	1.43	0.01	0.02	94.45
84	95-11	dacite	PR	219.4	68.20	0.19	18.27	3.36	0.04	5.42	1.01	0.92	2.91	0.02	100.50
87	95-11	basalt	PR	243.8	47.36	0.48	15.67	13.73	0.33	6.59	2.61	3.94	0.03	0.09	92.07
88	95-11	rhyolite	PR	253.3	62.88	0.12	20.45	3.07	0.04	6.70	2.41	1.23	3.31	0.01	100.42

Exploration and Mining Geology, Vol. 15, Nos. 3–4, p. 241–261, 2006

Table 1. (Continued)

Sample	Drillhole	Lithology	Fm.	Depth (m)	SiO_2 (wt.%)	TiO_2 (wt.%)	Al_2O_3 (wt.%)	$Fe_2O_3^T$ (wt.%)	MnO (wt.%)	MgO (wt.%)	CaO (wt.%)	Na_2O (wt.%)	K_2O (wt.%)	P_2O_5 (wt.%)	Total (wt.%)
89	95-11	rhyolite	PR	279.8	75.19	0.08	14.04	1.92	0.04	1.05	2.11	2.00	1.66	0.01	98.20
91	95-11	rhyolite	PR	323.7	76.69	0.09	14.91	2.08	0.04	2.12	3.14	1.25	1.44	0.01	101.89
92	95-11	rhyolite	PR	341.4	75.00	0.10	17.22	2.02	0.05	4.58	1.77	1.28	1.89	0.01	104.03
95	95-11	rhyolite	PR	351.2	70.93	0.10	14.05	0.53	0.14	0.77	6.22	2.38	2.08	0.05	97.48
98	95-11	black shale	PR	377.9	63.65	0.72	13.65	9.26	0.32	2.74	0.98	0.36	3.38	0.17	97.06
99	95-11	black shale	PR	381.2	67.96	0.70	14.08	5.67	0.07	2.64	0.93	0.08	4.33	0.09	99.61
102	95-11	dacite	PR	395.1	55.35	0.30	17.51	5.24	0.15	4.88	1.86	2.37	3.42	0.05	91.45
103	95-12	rhyolite	PR	15.3	75.86	0.10	12.13	2.31	0.11	0.42	0.98	4.18	0.62	0.02	96.82
107	95-12	gray mudstone	PR	20	62.09	0.76	15.96	9.18	0.77	3.06	0.91	1.30	3.34	0.04	97.90
110	95-12	dacite	PR	26.1	59.37	0.26	17.20	7.41	0.77	3.28	1.65	0.65	4.11	0.05	95.03
111	95-12	basalt	PR	37.7	47.05	0.58	17.44	12.40	0.66	7.38	1.84	4.86	0.51	0.09	93.00
115	95-12	rhyolite	PR	60.2	77.14	0.09	8.74	1.41	0.02	0.23	1.91	3.25	0.42	0.01	93.45
117	95-12	basalt	PR	64.2	41.83	0.31	13.53	13.14	0.26	10.20	4.82	3.45	0.12	0.04	87.86
118	95-12	basalt	PR	82.1	41.59	0.29	13.60	14.88	0.39	13.72	4.27	2.86	0.07	0.04	91.88
120	95-12	gray mudstone	PR	87.2	71.36	0.50	12.64	6.72	0.08	3.35	0.95	2.04	1.75	0.03	99.82
124	95-12	gray mudstone	PR	102.9	61.07	0.75	17.02	10.20	0.08	3.01	1.46	1.35	3.22	0.06	98.43
125	95-12	gray mudstone	PR	103.5	55.00	0.76	16.54	13.10	0.08	2.68	2.25	0.85	3.07	0.08	94.71
127	95-12	dacite	PR	107.7	67.95	0.21	15.14	5.00	0.11	4.01	2.28	1.64	2.28	0.05	99.48
128	95-12	rhyolite	PR	116.4	60.85	0.11	22.71	2.87	0.04	7.85	1.46	1.84	2.21	0.01	100.11
130	95-12	rhyolite	PR	144.2	72.32	0.07	16.28	2.46	0.04	2.64	1.75	1.54	2.64	0.01	99.89
131	95-12	rhyolite	PR	156	74.49	0.08	14.52	1.96	0.04	1.72	2.36	1.29	1.99	0.01	98.58
132	95-12	rhyolite	PR	187.9	60.94	0.08	22.05	2.84	0.05	6.43	1.00	1.72	2.59	0.01	97.87
133	95-12	rhyolite	PR	210.6	59.39	0.12	23.59	2.06	0.07	4.42	0.45	0.48	5.99	0.01	96.95
134	95-12	rhyolite	PR	213.1	54.07	0.13	17.18	2.04	0.46	1.75	15.27	1.64	3.84	0.01	96.83
138	95-12	black shale	PR	219.1	64.55	0.91	16.36	4.44	0.11	2.95	3.39	0.65	4.35	0.11	100.04
139	95-12	black shale	PR	222.7	69.97	0.82	15.73	4.08	0.10	2.84	1.94	0.65	4.10	0.10	102.25
141	95-12	dacite	PR	226.6	59.22	0.27	19.72	2.61	0.24	2.90	7.27	1.01	5.27	0.03	99.53
143	95-12	black shale	PR	230.1	77.19	0.49	12.00	3.83	0.09	2.39	1.45	0.61	2.95	0.08	102.92
146	95-12	dacite	PR	242.4	57.54	0.29	19.13	4.82	0.16	5.85	2.24	3.21	3.00	0.05	96.64
148	95-12	dacite	PR	269.7	62.55	0.24	14.19	3.21	0.07	3.09	4.50	3.82	1.54	0.05	93.69
150	95-12	dacite	PR	284.3	71.70	0.20	13.92	1.55	0.04	1.00	2.30	2.87	2.87	0.04	97.31
153	95-12	black shale	PR	289.1	63.69	0.81	16.34	5.11	0.03	3.00	1.67	0.16	5.18	0.08	100.92
155	95-12	black shale	PR	300	64.63	0.82	17.13	6.74	0.08	4.01	0.89	0.60	4.44	0.09	100.68
156	95-12	andesite	PR	304.5	46.40	0.37	21.23	10.69	0.11	6.40	5.70	0.26	6.16	0.12	97.74
158	95-12	andesite	PR	325.7	46.38	0.54	20.62	8.57	0.09	6.55	4.47	2.89	3.30	0.14	93.96
159	surface	gray mudstone	BL	0	62.27	0.82	16.86	12.49	0.41	3.19	0.43	0.59	2.92	0.24	100.46
160	surface	basalt	OM	0	44.63	0.66	13.55	13.51	0.20	10.66	5.91	1.21	1.55	0.33	92.44
161	surface	basalt	OM	0	50.58	0.68	13.83	13.55	0.17	11.62	3.61	1.27	1.12	0.16	96.80
162	surface	andesite	ER	0	52.57	0.37	16.57	9.52	0.17	6.11	3.03	5.92	0.14	0.07	94.56
166	surface	andesite	PR	0	49.55	0.50	16.38	11.53	0.58	7.59	1.26	4.48	0.08	0.09	92.14
167	surface	andesite	ER	0	59.77	0.85	19.83	11.16	0.56	2.82	1.08	0.26	4.28	0.14	101.00
168	surface	andesite	PR	0	42.26	0.36	15.49	10.77	0.13	12.35	3.60	3.19	0.57	0.22	89.80
169	surface	gray mudstone	BE	0	60.22	0.97	19.29	8.94	0.18	3.31	0.11	1.30	4.08	0.11	98.97

Table 1. (Continued)

Sample	Ba	S	Cr	Ni	Cu	Zn	Rb	Sr	Sc	Ga	V	Zr	Nb	Y	Zr/TiO_2	Nb/Y
	ppm	ppm	ppm	ppm	ppm	ppm	ppm	ppm	ppm	ppm	ppm	ppm	ppm	ppm		
1	322	226	13	<LD	10	20	38	266	<LD	10	25	159	11.3	24.1	0.043	0.47
3	721	522	27	<LD	12	25	44	115	14	13	63	141	10.5	22.0	0.037	0.48
6	336	236	54	<LD	42	43	11	148	32	16	203	76	5.5	14.8	0.018	0.37
7	401	858	68	<LD	31	37	26	167	24	15	146	79	5.4	15.2	0.023	0.35
10	876	448	46	13	34	46	152	293	18	20	110	125	12.9	25.4	0.019	0.51
14	377	191	28	<LD	97	51	29	173	40	15	427	31	2.1	10.2	0.007	0.21
15	544	1125	85	32	45	41	133	154	22	19	131	132	16.2	26.9	0.018	0.60
16	532	191	41	6	40	40	86	472	21	16	170	65	4.7	17.5	0.017	0.27
17	568	768	79	24	44	44	154	38	14	22	150	134	16.7	24.3	0.017	0.69
18	563	1678	97	22	44	43	132	103	19	21	167	130	15.6	30.3	0.018	0.51
20	133	881	160	26	57	37	12	207	36	14	268	26	1.9	8.3	0.007	0.22
21	138	246	156	36	68	39	10	315	40	15	301	29	1.7	9.4	0.007	0.18
24	620	513	79	27	44	41	97	129	20	23	143	128	15.9	39.4	0.018	0.40
26	47	945	25	<LD	26	33	<LD	98	23	14	211	51	2.2	13.3	0.016	0.16
29	151	771	20	<LD	17	30	4	106	20	9	162	48	2.2	11.5	0.014	0.19
30	338	6343	24	<LD	33	44	8	318	35	13	257	46	2.3	14.7	0.011	0.15
31	176	168	12	<LD	38	34	3	187	38	13	208	53	2.1	11.9	0.014	0.18
32	640	200	87	40	41	43	117	72	14	20	169	161	18.3	26.5	0.022	0.69
37	580	134	81	23	33	44	111	121	16	24	130	165	18.5	27.8	0.019	0.67
39	561	107	97	35	26	53	169	53	19	28	157	174	19.7	42.7	0.019	0.46
40	666	101	100	45	27	47	187	40	22	26	183	165	21.4	29.5	0.018	0.73
42	97	235	22	<LD	23	48	<LD	81	31	17	205	43	2.7	13.9	0.010	0.19
48	213	616	240	15	103	54	2	97	47	8	224	19	1.1	12.6	0.009	0.09
50	1955	93	<LD	<LD	31	45	66	140	13	10	9	134	6.7	29.3	0.089	0.23
53	1331	13011	113	33	74	317	80	61	10	17	625	148	16.9	32.7	0.021	0.52
55	1376	249	73	52	41	39	42	691	17	21	185	139	6.9	13.4	0.025	0.51
56	1236	356	79	53	18	57	37	1056	18	27	160	124	5.2	8.6	0.020	0.60
57	1817	3982	92	24	72	30	80	123	17	21	279	173	16.1	26.0	0.023	0.62
58	28	712	19	<LD	30	65	1	133	20	13	175	52	2.1	13.0	0.013	0.16
59	194	2255	15	<LD	52	187	9	143	25	16	184	101	3.3	17.8	0.025	0.19
62	51	111	15	<LD	32	37	<LD	188	24	10	197	48	2.9	12.6	0.012	0.23
66	98	140	<LD	<LD	24	69	2	117	39	18	393	32	1.4	13.8	0.005	0.11
67	390	106	<LD	<LD	<LD	<LD	33	65	18	8	11	43	2.5	6.0	0.016	0.42
69	226	98	<LD	<LD	5	24	28	47	12	7	16	51	2.3	8.9	0.023	0.26
72	634	81	236	12	14	91	107	234	46	19	142	35	1.7	13.6	0.012	0.12
74	41	318	61	19	104	40	4	54	39	10	279	18	<LD	4.5	0.008	0.11
75	49	211	104	17	96	39	3	147	42	13	314	23	<LD	8.1	0.008	0.06
76	333	71	<LD	<LD	<LD	<LD	30	102	13	11	9	126	6.1	28.0	0.099	0.22
78	114	253	222	28	113	29	<LD	150	47	12	279	13	<LD	7.3	0.004	0.07
79	388	177	207	29	69	29	<LD	282	40	10	278	16	1.2	6.3	0.005	0.20
81	172	209	<LD	<LD	5	70	<LD	76	<LD	6	18	89	4.2	23.9	0.082	0.18
82	2137	98	<LD	<LD	5	38	38	197	12	19	8	220	17.5	64.2	0.227	0.27
83	<LD	246	196	24	124	37	<LD	274	41	12	271	15	<LD	6.3	0.005	0.08
84	643	120	<LD	<LD	26	100	66	118	15	14	11	146	7.3	35.5	0.076	0.21
87	28	4309	142	23	35	60	<LD	168	50	16	469	13	1.1	13.0	0.003	0.08
88	564	78	<LD	<LD	<LD	28	69	386	17	20	<LD	227	17.2	62.7	0.183	0.27

Table 1. (Continued)

Sample	Ba ppm	S ppm	Cr ppm	Ni ppm	Cu ppm	Zn ppm	Rb ppm	Sr ppm	Sc ppm	Ga ppm	V ppm	Zr ppm	Nb ppm	Y ppm	Zr/TiO_2	Nb/Y
89	338	57	<LD	<LD	6	6	36	174	10	12	<LD	158	11.7	41.4	0.205	0.28
91	255	76	<LD	<LD	6	11	36	270	16	12	<LD	169	12.9	41.8	0.197	0.31
92	253	85	<LD	<LD	7	12	43	199	19	13	<LD	183	13.6	46.1	0.189	0.30
95	992	246	<LD	<LD	<LD	<LD	38	174	15	7	<LD	145	10.7	35.1	0.147	0.31
98	3696	5037	140	19	79	93	108	34	17	17	238	144	17.6	35.8	0.020	0.49
99	3737	9411	70	40	77	215	134	22	15	15	936	130	16.3	33.6	0.019	0.48
102	1443	255	30	10	22	21	79	276	16	19	93	155	16.4	32.4	0.052	0.51
103	175	38	<LD	<LD	<LD	52	13	76	<LD	11	<LD	145	8.8	33.9	0.147	0.26
107	754	1099	90	33	24	44	119	45	18	25	133	138	17.5	26.3	0.018	0.67
110	1654	47	<LD	<LD	15	41	127	233	20	16	26	129	6.5	25.5	0.050	0.26
111	540	37	22	<LD	70	63	14	175	52	15	333	31	2.5	13.3	0.005	0.19
115	217	592	13	<LD	7	<LD	10	233	<LD	7	8	133	8.3	18.3	0.142	0.45
117	139	181	69	17	93	47	2	137	49	10	318	29	2.0	11.2	0.009	0.18
118	81	204	108	31	114	44	1	122	58	11	293	25	1.8	9.9	0.009	0.18
120	572	1107	56	9	33	27	57	89	11	14	89	104	13.0	21.9	0.021	0.60
124	769	76	86	20	30	42	112	51	14	23	135	137	19.1	28.1	0.018	0.68
125	785	257	94	22	12	49	106	337	12	24	129	143	19.5	28.4	0.019	0.69
127	713	2468	<LD	<LD	47	196	62	107	17	14	23	78	4.8	26.2	0.038	0.18
128	432	38	<LD	<LD	-1	32	51	288	14	23	<LD	243	18.0	55.9	0.219	0.32
130	620	38	<LD	<LD	2	19	69	140	11	15	<LD	186	12.8	42.2	0.286	0.30
131	386	64	<LD	<LD	10	11	41	92	<LD	12	<LD	167	12.8	40.9	0.222	0.31
132	622	52	<LD	<LD	2	24	62	170	13	19	6	227	16.6	61.1	0.270	0.27
133	2494	67	<LD	<LD	4	24	164	35	19	21	<LD	244	17.6	61.5	0.205	0.29
134	2886	257	<LD	<LD	7	21	98	188	27	11	<LD	173	12.3	33.9	0.139	0.36
138	3343	6592	83	16	41	44	131	109	15	19	473	221	19.6	35.4	0.024	0.55
139	3076	5621	72	16	37	44	121	60	21	16	422	202	18.1	32.1	0.024	0.56
141	4891	1445	22	<LD	9	<LD	134	140	26	13	78	128	9.6	20.3	0.047	0.47
143	2001	5890	54	18	35	87	86	44	10	12	463	107	12.8	25.7	0.022	0.50
146	1715	241	24	5	24	21	76	249	22	22	94	158	18.2	35.1	0.054	0.52
148	981	986	26	<LD	20	13	29	165	22	13	58	131	14.3	31.5	0.054	0.45
150	2691	1763	21	<LD	26	4	55	241	11	7	50	109	12.8	25.4	0.054	0.50
153	4903	16 204	86	58	62	85	143	31	22	16	710	167	20.2	38.4	0.021	0.53
155	1898	3477	112	35	59	81	106	32	20	21	236	177	19.8	35.4	0.021	0.56
156	1793	93	43	30	19	43	118	85	19	19	217	99	5.8	9.3	0.027	0.62
158	1624	108	48	38	44	33	64	864	21	24	217	113	5.1	10.3	0.021	0.50
159	869	129	80	24	10	46	114	56	18	21	114	134	16.3	30.9	0.016	0.53
160	575	47	40	<LD	142	43	42	348	35	14	284	97	8.1	24.8	0.015	0.33
161	424	34	39	9	185	50	28	286	24	15	285	108	8.8	19.1	0.016	0.46
162	67	83	41	<LD	39	65	3	79	34	17	189	51	2.7	14.0	0.014	0.19
166	45	135	<LD	<LD	5	93	2	172	35	14	84	59	3.2	26.2	0.012	0.12
167	880	30	91	41	42	52	178	28	21	25	157	170	20.0	35.1	0.020	0.57
168	5885	71	128	96	111	39	9	423	20	11	215	101	4.0	14.1	0.028	0.28
169	678	991	106	30	25	37	169	29	24	22	128	179	19.4	27.3	0.018	0.71

Notes

Depth of drillhole samples is represented as a downhole depth. Formational units (Fm.): BE = Bright Eye Brook, BL = Belle Lake, PR = Porten Road, ER = Eel River, OM = Oak Mountain, <LD = below instrumental detection limit.

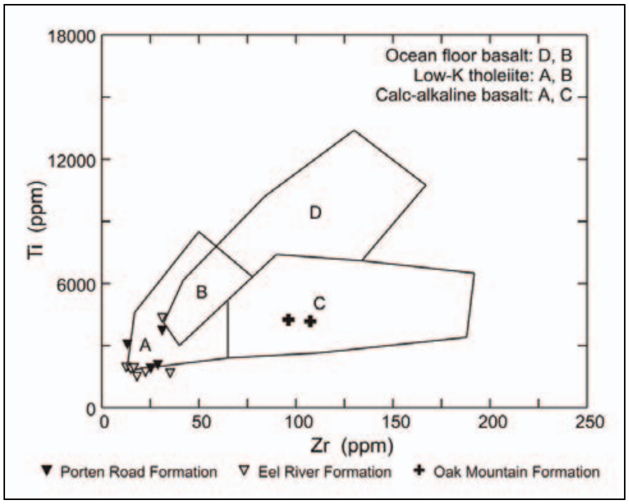

Fig. 10. Ti vs. Zr discrimination diagram for basaltic rocks, after Pearce and Cann (1973), illustrating the strongly calc-alkaline nature of Oak Mountain basalt, compared to more tholeiitic affinities of basalts from the Porten Road and Eel River formations.

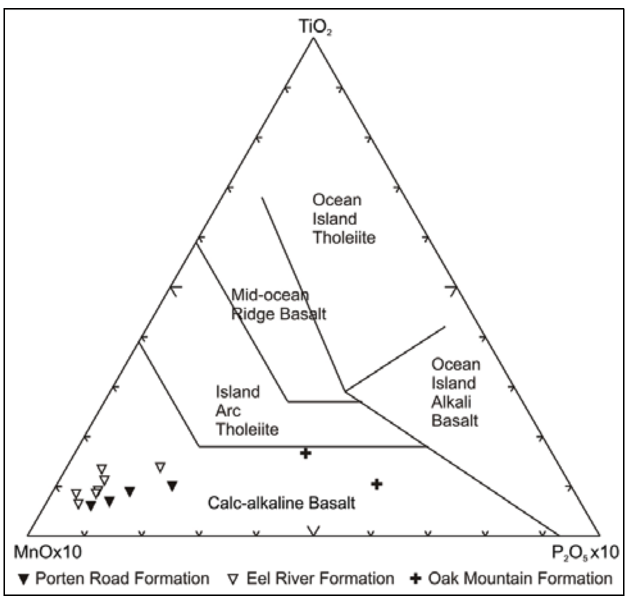

Fig. 11. $MnO–TiO_2–P_2O_5$ discrimination diagram, after Mullen (1983), for basaltic rocks (45–54 wt.% SiO_2) from the Porten Road, Eel River, and Oak Mountain formations.

Volcanic Chemostratigraphy

Porten Road Formation

Intermediate hyaloclastite overlying sedimentary rocks of the Bright Eye Brook Formation at the base of the Porten Road Formation represent the earliest known volcanism in the Eel River area (Fig. 4). The most distinguishing features of this intermediate hyaloclastite (samples 55, 56, 156, 158, 166, 168) are the low Zr/TiO_2 (0.012–0.028) and high Nb/Y (0.12–0.62) ratios (Fig. 12a,c). Despite the low silica contents (42.26–54.73 wt.% SiO_2) of the altered fragments, all of the fragment analyses plot within the field for andesite on a plot of Zr/TiO_2 versus Nb/Y (Fig. 9). Overlying the intermediate breccia is a porphyritic autobreccia that is dacitic in composition (samples 141, 146, 148, 150, 102). Analysis of altered fragments reveals variable SiO_2 contents ranging from 55.4 to 71.7 wt.%. The Zr/TiO_2 content of the autobreccia is higher than the underlying intermediate hyaloclastite and ranges from 0.047 to 0.054 (Fig. 12b,c). Nb/Y displays little variation with slightly lower values than the intermediate hyaloclastite, ranging from 0.45 to 0.52 (Table 1). The dacite autobreccia is overlain by black shale, which is in turn overlain by a thick sequence of felsic breccias that are rhyolite in composition (samples 88, 89, 91, 92, 95, 128, 130, 131, 132, 133, 134). The Zr/TiO_2 of the rhyolite is higher than that of the preceding units (Fig. 12b,c), ranging from 0.139 to 0.286, whereas Nb/Y is slightly lower with an average of 0.30, ranging from 0.27 to 0.36 (Table 1).

The upper part of the Porten Road Formation is characterized by the first appearance of mafic volcanic rocks in the Meductic Group. The unit of massive basalt (samples 117, 118) is similar in composition to basalt from the overlying Eel River Formation, and can be distinguished in part by its slightly higher P_2O_5 (0.04 wt.%) content and higher Nb/Y (~0.18; Fig. 12b,c). The eruption of basalt likely triggered debris flows resulting in diverse polylithic fragmental rocks. These volcaniclastic rocks contain fragments of rhyolite (samples 103, 115), dacite (76, 110, 127), and basalt (87, 111), which are presumably derived from the underlying massive basalt, rhyolite breccia, and dacite autobreccia bodies, based on Nb/Y and Zr/TiO_2 ratios (Fig. 12b,c). However, some of the fragments display ratios falling outside the ranges documented in the underlying units, most likely due to lateral variations within the volcanic pile.

Eel River Formation

Volcanic rocks in the Eel River Formation include mafic to intermediate volcaniclastic rocks, massive basalt, and lesser dacite breccia. Zr/TiO_2 and Nb/Y ratios allow Eel River volcanic rocks to be distinguished from those in the Porten Road Formation. Volcanic rocks belonging to the Eel River Formation typically have lower Zr/TiO_2 ratios between 0.004 and 0.043, whereas the Nb/Y ratio has a similar range of values as the Porten Road volcanic rocks (Fig. 9).

Near the base of the Eel River Formation, massive basalt (samples 79, 83) directly overlies felsic breccias of the Porten Road Formation. This basalt can be distinguished from its Porten Road counterpart by lower P_2O_5 contents and a generally lower Nb/Y ratio (Fig. 12b,c).

The massive basalt is overlain by polylithic fragmental rocks containing fragments of basalt (samples 72, 74, 75) and dacite (samples 67, 69), interstratified with ferromanganiferous mudstone. The dacite fragments display a lower Zr/TiO_2 ratio (0.016–0.023) than felsic volcanic rocks of the Porten Road Formation; Nb/Y ranges from 0.26 to 0.42

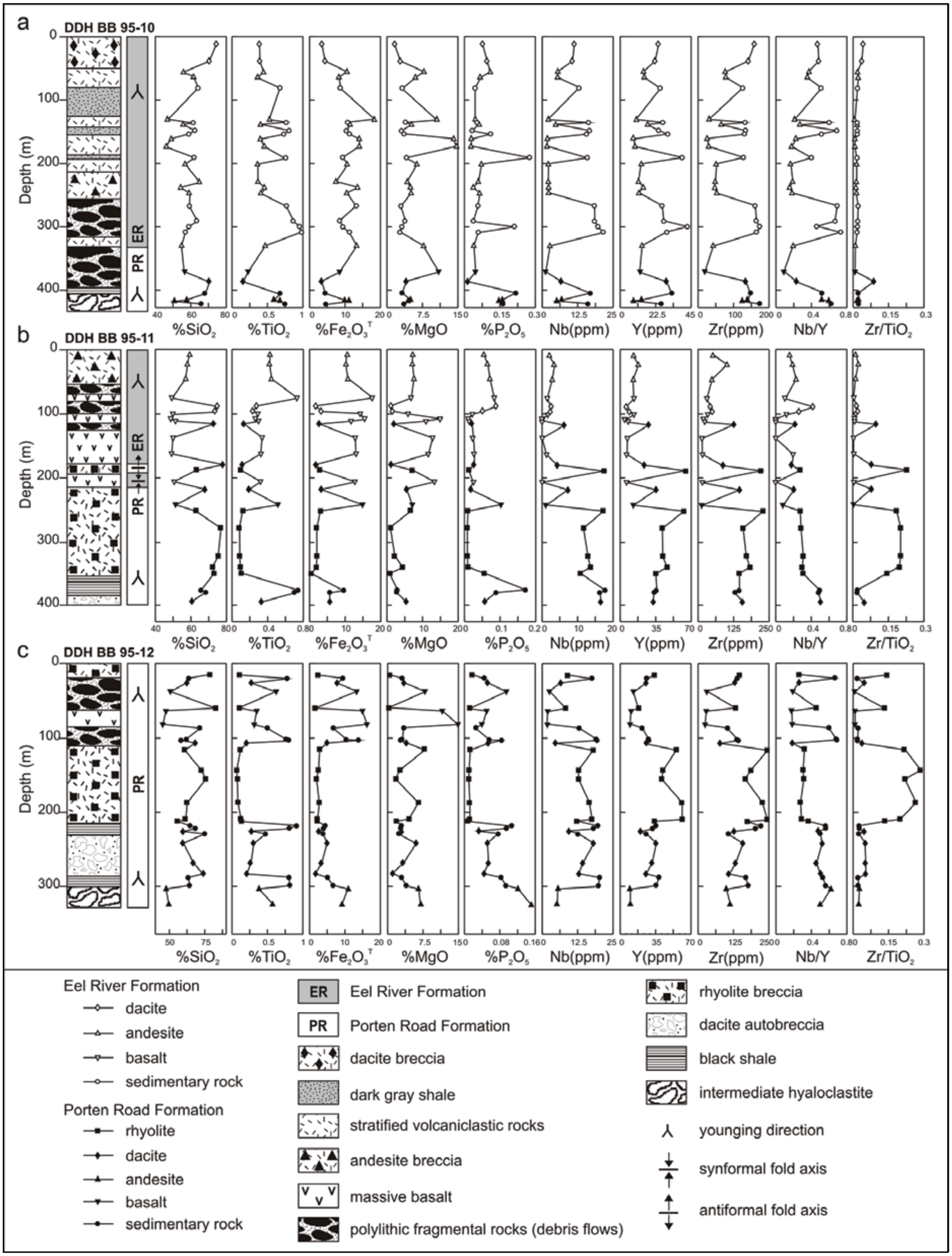

Fig. 12. Major and trace element compositional profiles for three drillhole intersections: ***a.*** DDH BB 95-10, collared in reworked dacite breccia (Eel River Formation) and transecting a thick, graded volcaniclastic sequence before passing into debris flows of the Porten Road Formation; ***b.*** DDH BB 95-11, collared in reworked intermediate breccia (Eel River Formation) and intersecting a sharp boundary with the underlying Porten Road Formation; ***c.*** DDH BB 95-12, collared in reworked felsic breccia of the Porten Road Formation and intersecting a near complete stratigraphic succession of the Porten Road Formation.

(Fig. 12b). The low Zr/TiO_2 ratio indicates that these fragments did not originate in the underlying Porten Road Formation, but are coeval with Eel River volcanism.

The above unit is overlain by a thick sequence of graded mafic to intermediate volcaniclastic rocks (samples 6, 7, 14, 16, 20, 21, 26, 29, 30, 31, 42). The SiO_2 content varies widely from 41.9 to 61.2 wt.%, and $Fe_2O_3^T$ averages 11.0 wt.% with a range of 7.0 to 16.5 wt.% (Fig. 12a). However, these intermediate rocks are distinguished by their low Zr/TiO_2 ratio, which ranges from 0.007 to 0.023. The Nb/Y ratio of Eel River volcaniclastic rocks averages 0.23 (0.15–0.37), whereas the Porten Road intermediate hyaloclastite averages 0.44 (Table 1).

In the upper part of the Eel River Formation, intermediate volcaniclastic rocks are overlain by felsic breccia (samples 1, 3) that is dacitic in composition. Silica ranges from 69.5 to 71.5 wt.% SiO_2 with a distinctively low Zr/TiO_2 ratio, ranging from 0.037 to 0.043, whereas the Nb/Y ratio varies from 0.47 to 0.48 (Fig. 12a).

Sedimentary Chemostratigraphy

Porten Road Formation

Sedimentary rocks occur throughout the Porten Road Formation in polylithic fragmental rocks, as discrete bands, and as thick accumulations marking breaks in volcanic activity. In the lower part of the Porten Road Formation, black shale occurs in two units (samples 53, 98, 99, 138, 139, 143, 153, 155) separating three compositionally distinct volcanic packages (Fig. 12c). The black shale was deposited during extended periods of oceanic anoxia, which also occurred during deposition of the underlying Bright Eye Brook Formation (Dostal, 1989). Silica in the black shale averages 67.8 wt.% with a range of 63.7 to 77.2 wt.% SiO_2, reflecting variable clay versus quartz content. $Fe_2O_3^T$ averages 5.47 wt.%, ranging from 3.83 to 9.26 wt.%, and covaries with clay mineral abundance. A strong Spearman Rank correlation exists between Al_2O_3 and many trace elements, including Zr ($r' = 0.86$; Fig. 13a). Black shale in the Porten Road Formation has a more evolved source than dark gray shale from either the Porten Road and Eel River formations based on Zr, Nb, and Ba abundances (Table 1). Coincident with low-MnO contents, the Porten Road black shale exhibits geochemical features consistent with stagnant reducing ocean conditions, reflected in higher average contents of Ba (2998 ppm), Cu (58 ppm), Zn (121 ppm), S (8155 ppm), and V (513 ppm; Fig. 13b).

In the upper part of the Porten Road Formation, dark gray shale and fine-grained wacke (Fig. 12a; samples 57, 107, 120, 124, 125) occur in thin beds and in the matrix of many polylithic fragmental rocks (Fig. 12c). Silica in these shales averages 63.2 wt.% (55.0–71.4 wt.%) and $Fe_2O_3^T$ averages 8.77 wt.% (4.64–13.10 wt.%). These sedimentary rocks, deposited under more oxic conditions, contain less Ba (939 ppm), Cu (34 ppm), Zn (38 ppm), S (1304 ppm), and V (153 ppm) than the underlying black shale (Table 1). The dark gray shale exhibits a poor correlation with black shales from the lower Porten Road Formation (Fig. 13), but is chemically similar to the Bright Eye Brook Formation (Hennessy and Mossman, 1996).

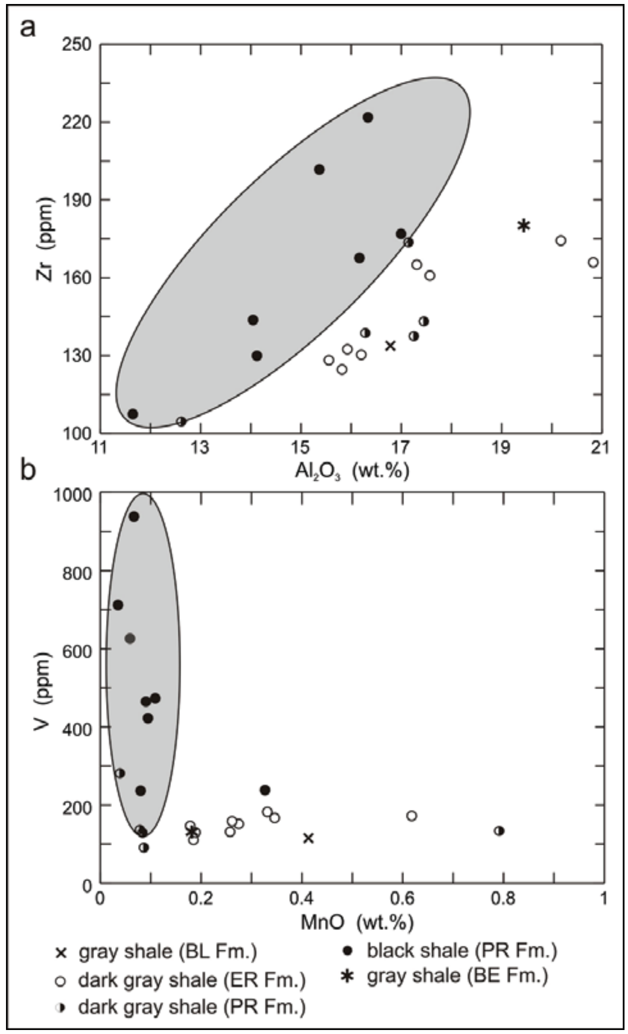

Fig. 13. ***a.*** Zr vs. Al_2O_3, and ***b.*** V vs. MnO plots illustrating different geochemical profiles for black shale and gray shale from the Bright Eye Brook (BE), Porten Road (PR), Eel River (ER), and Belle Lake (BL) Formations. Gray shaded regions show field of Porten Road black shales.

Eel River Formation

Black shale is absent in the Eel River Formation, where sedimentary rocks consist of dark gray shale and fine-grained wacke, suggesting that more oxic conditions prevailed (Fig. 12a). Dark gray shale is interbedded with intermediate volcaniclastic rocks forming thinly layered turbidite sequences in what is interpreted as a more distal environment. Silica in these mudstones (samples 10, 15, 17, 18, 24, 32, 37, 39, 40) averages 59.1 wt.% (55.1–63.1 wt.%), whereas $Fe_2O_3^T$ averages 10.0 wt.% (8.50–12.61 wt.%). The contents of Ba (624 ppm), Cu (38 ppm), Zn (45 ppm), S (564 ppm), and V (149 ppm) are similar to dark gray shale in the upper parts of the Porten Road Formation, and are lower than Porten Road black shale (Table 1). Like the Porten Road gray shales, a strong Spearman Rank correlation exists between Al_2O_3 and Zr ($r' = 0.93$) for dark gray shales of the Eel River Formation (Fig. 13a).

Discussion and Conclusions

Stratigraphy of the Eel River Area

Detailed logging of exploration drillholes in the Benton Road area has greatly improved the understanding of the stratigraphy of the Porten Road and Eel River formations. Several laterally continuous units were identified in drillhole sections, allowing investigation of lateral variations in stratigraphy. The intermediate hyaloclastite and overlying black shale at the base of the Porten Road Formation appear to be laterally continuous for over 1500 m along strike. However, the abundance and characteristics of the overlying felsic volcanic rocks were found to be highly variable and partly controlled by their proximity to a felsic dome (intersected in DDH BB 94-7; Williamson, 1996) to the northeast. Proximal to this volcanic center, felsic autobreccias and flows are voluminous and exhibit less reworking than distal felsic volcanic rocks to the southwest.

The upper section of the Porten Road Formation marks the transition to more oxidizing conditions, signaled by the appearance of gray shale and absence of black shale. Mafic volcanic flows and breccias make their first appearance in this upper section and are indistinguishable from their Eel River counterparts. This section is also characterized by numerous polylithic fragmental rocks, interpreted as debris flows triggered by eruptive events and/or accumulation of volcanic material to the point of instability. Examination of fragments indicate that they most likely originate from underlying felsic breccias and flows of the Porten Road Formation.

Volcanic and sedimentary rocks of the Eel River Formation also display characteristics indicative of a proximal–distal transition. In the northeast, massive basalt is overlain by polylithic fragmental rocks and intermediate breccia. However, in distal portions of the system, mafic fragmental rocks are overlain by a thick sequence of graded mafic to intermediate volcaniclastic rocks (overall, andesitic in composition) interbedded with mudstone. These debris flows are interpreted as lateral equivalents of the intermediate breccia. Equally important is the presence of a unit of dacite breccia towards the top of the Eel River Formation. The apparent transition from massive basalt and andesite to a dacite breccia indicate that fractional crystallization may be responsible for the upward evolving nature of the volcanic pile.

Chemostratigraphy

Volcanic rocks belonging to the Meductic Group have undergone a low grade of metamorphism. However, due to alteration, most major elements do not represent the original composition of the volcanic rock. Spilitization of basalts during eruption on the seafloor has resulted in a net gain of Na_2O. Volcanic rocks have undergone varying amounts of chloritic alteration resulting in variations in $Fe_2O_3^T$ and MgO. The mobility of SiO_2 has led to silica loss and gain in samples. As a result, immobile elements are relied upon for lithology.

Overall, geochemical results indicate a general decrease in the SiO_2 content of volcanic rocks in order of eruption from the dominantly felsic Porten Road Formation to the mafic and intermediate volcanic rocks of the Eel River Formation. However, progressive fractional crystallization of the magmas is substantiated by a general increase in Zr/TiO_2 with increasing SiO_2 (Fig. 12) in both the Porten Road and Eel River formations. Furthermore, Zr/TiO_2 and Nb/Y ratios allow felsic and intermediate units of the Porten Road Formation to be distinguished from those in the Eel River Formation. Zr/TiO_2 and Nb/Y ratios of fragments in polylithic fragmental rocks of the Porten Road Formation indicate that they originate from underlying autobreccias, and flows.

Basalt from the Eel River Formation may be distinguished from Porten Road basalt by its lower contents of P_2O_5 and lower Nb/Y; otherwise they are indistinguishable. Chemical similarities between basalts at the top of the Porten Road Formation and base of the Eel River Formation indicate that they are probably genetically related. The Oak Mountain basalt has a strong calc-alkaline signature with higher contents of TiO_2, P_2O_5, Zr, and Nb than basalt from the Eel River and Porten Road formations (Figs. 10, 11).

During breaks in volcanic activity, black shale was deposited under anoxic conditions, which prevailed during emplacement of the lower part of the Porten Road Formation. Dark gray shale and wacke near the top of the Porten Road Formation and throughout the Eel River Formation reflect a change to more oxidizing conditions. The geochemical composition of the shales reflects their lithological differences, with black shale having higher contents of Ba, S, Cu, Zn, and V, and markedly different trends on variation diagrams (Fig. 13).

Economic Potential

The economic potential of the Eel River area is encouraging. The Bald Mountain massive sulfide deposit in northern Maine is hosted by a sequence of basalt, andesite, rhyolite, volcaniclastic, and fragmental rocks (Scully, 1993) similar to the Eel River volcanic suite. Furthermore, gold-bearing base metal massive sulfide clasts have been found in intermediate volcanic rocks near Monument Brook in eastern Maine. Mineralization in the Eel River area consists of thin lenses and fragments of massive pyrrhotite and pyrite with lesser sphalerite and chalcopyrite, hosted by felsic volcanic and sedimentary rocks of the Porten Road Formation. Hydrothermal systems were active during emplacement of

Porten Road felsic volcanic rocks following deposition of the upper black shale unit. The accumulation of black shales between distinct volcanic units indicates a significant pause in volcanism. This would have allowed for the establishment of hydrothermal convection cells and an evolved hydrothermal system. Massive sulfides likely accumulated on the seafloor surrounding active hydrothermal vents, proximal to emerging felsic domes. Anoxic water conditions, which prevailed during the deposition of black shale and sulfides, prevented oxidation and allowed for the preservation of stratiform massive sulfide lenses. In the southwest, distal to the volcanic center, the intermediate hyaloclastite at the base of the Porten Road Formation is overlain by an attenuated unit of felsic volcaniclastic rocks and debris flows locally containing sulfide clasts. The polylithic nature of the fragmental rocks containing black shale, rhyolite, dacite, basalt, and lesser andesite, indicate scouring of various rock types on the seafloor during transport. Consolidated sulfides occurring in an unstable topographic position may be transported long distances provided that relief is significant. For example, in the Buchans area, debris flows were triggered by caldera resurgence accompanied by gaseous and/or phreatomagmatic eruptions (Kirkham and Thurlow, 1987). Many of the rocks of the Meductic Group were likely emplaced as debris flows initiated by the submarine eruption of volcanic material.

The transition from a proximal setting characterized by a felsic dome and abundant autobreccia in the northeast to mixed fragmental and volcaniclastic rocks in the southwest (Fig. 4) may explain the presence of massive sulfide fragments in debris flows along the Benton Road; stratiform sulfides 1500 m to the northeast are a possible source. Unfortunately, drillhole BB 95-11, which intersects felsic autobreccias and flows between the apparent source region and the Benton Road occurrence, contains only minor sulfide fragments. Therefore the source of massive sulfide clasts may instead lie to the north at depth or to the northeast along strike.

The occurrence of ore-bearing debris flows near Buchans, Newfoundland, illustrates the economic potential of transported ores, both as economic deposit and as an exploration tool in tracing their source (Kirkham and Thurlow, 1987). The sulfide clasts in drillholes intersecting distal parts of the Porten Road Formation and in the Benton Road occurrence support the syn-volcanic transport of clasts in debris flows. Hence, further economic potential may exist to the northeast in a more proximal setting.

Acknowledgments

The New Brunswick Department of Natural Resources (NBDNR) and a NSERC grant to D.R. Lentz financially supported this investigation. The staff of the Sussex branch of NBDNR provided logistical support during the summer sampling program. This manuscript benefited from extensive reviews by R. Wilson, J.P. Richards, and an anonymous reviewer.

References

Bailey, L.W., 1901, On some geological correlations in New Brunswick: Royal Society of Canada, Transactions, v. 7, p. 143–150.

Bourque, P.-A., Brisebois, D., and Malo, M., 1995, Gaspé Belt, *in* Williams, H., ed., Geology of the Appalachian-Caledonian Orogen in Canada and Greenland: Geological Survey of Canada, Geology of Canada, no. 6, p. 316–351.

Cas, R.A.F., 1992, Submarine volcanism: Eruption styles, products, and relevance to understanding the host-rock successions to volcanic-hosted massive sulfide deposits: Economic Geology, v. 87, p. 511–541.

Dostal, J., 1989, Geochemistry of Ordovician volcanic rocks of the Tetagouche Group of southwestern New Brunswick: Atlantic Geology, v. 25, p. 199–209.

Fyffe, L.R., 1994, A note on the geochemistry of some shales from the Bathurst-Newcastle Mining Camp, northern New Brunswick, Canada: Atlantic Geology, v. 30, p. 143–151.

Fyffe, L.R., 1999, Geology of the Eel River area (part of NTS 21G/13h), York and Carleton counties, New Brunswick: New Brunswick Department of Natural Resources and Energy, Minerals and Energy Division, Plate 99-30.

Fyffe, L.R., 2001, Stratigraphy and geochemistry of the Ordovician volcanic rocks of the Eel River area, west-central New Brunswick: Atlantic Geology, v. 37, p. 81–101.

Fyffe, L.R., and Fricker, A., 1987, Tectonostratigraphic terrane analysis of New Brunswick: Maritime Sediments and Atlantic Geology, v. 23, p. 113–123.

Fyffe, L.R., and Pickerill, R.K., 1993, Geochemistry of Upper Cambrian-Lower Ordovician black shale along a northeastern Appalachian transect: Geological Society of America Bulletin, v. 105, p. 897–910.

Fyffe, L.R., and Swinden, H.S., 1992, Paleotectonic setting of Cambro-Ordovician volcanic rocks in the Canadian Appalachians: Geoscience Canada, v. 18, p. 145–157.

Fyffe, L.R., Forbes, W.H., and Riva, J., 1983, Graptolites from the Benton area of west-central New Brunswick and their regional significance: Maritime Sediments and Atlantic Geology, v. 19, p. 117–125.

Galley, A.G., 1995, Target vectoring using lithogeochemistry: Applications to the exploration of volcanic-hosted massive sulphide deposits: CIM Bulletin, v. 88, p. 15–27.

Goodfellow, W.D., and McCutcheon, S.R., 2003, Geological and genetic attributes of volcanic sediment-hosted massive sulfide deposits of the Bathurst Mining Camp, northern New Brunswick—A synthesis: Economic Geology, Monograph 11, p. 245–301.

Hennessy, J.F., and Mossman, D.J., 1996, Geochemistry of Ordovician black shales at Meductic, southern Miramichi Highlands, New Brunswick: Atlantic Geology, v. 32, p. 233–245.

Hughes, C.J., 1972, Spilites, keratophyres, and the igneous spectrum: Geological Magazine, v. 109, p. 513–527.

Irvine, T.N., and Baragar, W.R.A., 1971, A guide to the chemical classification of the common volcanic rocks: Canadian Journal of Earth Sciences, v. 8, p. 523–548.

Kirkham, R.V., and Thurlow, J.G., 1987, Evaluation of a resurgent caldera and aspects of ore deposition and deformation: Geological Survey of Canada, Report 10, Paper 86-24, p. 177–194.

Le Bas, M.J., Le Maitre, R.W., Streckeisen, A., and Zanettin, B., 1986, A chemical classification of volcanic rocks based on the total alkali-silica diagram: Journal of Petrology, v. 27, p. 745–750.

Lentz, D.R., 1995, Preliminary evaluation of six in-house rock geochemical standards from the Bathurst Camp, New Brunswick: New Brunswick Department of Natural Resources and Energy, Miscellaneous Report 18, p. 81–89.

Lentz, D.R., Goodfellow, W.D, and Brooks, E., 1996, Chemostratigraphy and depositional environment of an Ordovician sedimentary section across the Miramichi Group-Tetagouche Group contact, northeastern New Brunswick: Atlantic Geology, v. 32, p. 101–122.

Longerich, H.P., 1995, Analysis of pressed pellets of geological samples using wavelength-dispersive X-ray fluorescence spectrometry: X-Ray Spectrometry, v. 24, p. 123–136.

McClay, K.R., and Ellis, P.G., 1983, Deformation and recrystallization of pyrite: Mineralogical Magazine, v. 47, p. 527–538.

Mullen, E.D., 1983, $MnO/TiO_2/P_2O_5$: A minor element discriminant for basaltic rocks of oceanic environments and its implications for petrogenesis: Earth and Planetary Science Letters, v. 62, p. 53–62.

Neuman, R.B., 1984, Geology and paleobiology of islands in the Ordovician Iapetus Ocean: Review and implications: Geological society of America Bulletin, v. 95, p. 1188–1201.

O'Brien, B.H., 1977, Pre-Acadian deformation, metamorphism, and intrusion in the vicinity of the Pokiok pluton, west-central New Brunswick, and its regional implications: Canadian Journal of Earth Sciences, v. 14, p. 1796–1808.

Pearce, J.A., and Cann, J.R., 1973, Tectonic setting of basic volcanic rocks determined using trace element analysis: Earth and Planetary Science Letters, v. 19, p. 290–300.

Pickerill, R.K., and Fyffe, L.R., 1999, The stratigraphic significance of trace fossils from the Lower Paleozoic Baskahegan Lake Formation near Woodstock, west-central New Brunswick: Atlantic Geology, v. 35, p. 215–224.

Scully, M.V., 1993, The Bald Mountain massive-sulfide deposit, Aroostook County, Maine, *in* McCutcheon, S.R., ed., Lower Paleozoic VMS deposits of Maine: Geological Society of the Canadian Institute of Mining, Metallurgy, and Petroleum, Bathurst '93, 3rd Annual Field Conference, 1993, Proceedings, p. 35–44.

van Staal, C.R., 1987, Tectonic setting of the Tetagouche group in northern New Brunswick: Implications for plate tectonic models of the northern Appalachians: Canadian Journal of Earth Sciences, v. 24, p. 1329–1351.

van Staal, C.R., 1994, Brunswick subduction complex in the Canadian Appalachians: Record of the Late Ordovician to Late Silurian collision between Laurentea and the Gander margin of Avalon: Tectonics, v. 13, p. 946–962.

van Staal, C.R., and Fyffe, L.R., 1995a, Dunnage Zone, New Brunswick: Geological Survey of Canada, Geology of Canada, no. 6, p. 166–178.

van Staal, C.R., and Fyffe, L.R., 1995b, Gander Zone, New Brunswick: Geological Survey of Canada, Geology of Canada, no. 6, p. 216–223.

Venugopal, D.V., 1978, Geology of Benton-Kirkland, Upper Eel River Bend, map area G-22 (21 G/13): New Brunswick Department of Natural Resources, Mineral Resources Branch, Map Report 78-3, 16 p.

Venugopal, D.V., 1979, Geology of Debec Junction-Gibson Millstream-Temperance Vale-Meductic region, map areas G-21, H-21, I-21, and H-22 (Parts of 21 J/3, 21 J/4, 21G/13, 21 G/14): New Brunswick Department of Natural Resources, Mineral Resources Branch, Map Report 79-5, 36 p.

Williams, H., 1979, Appalachian Orogen in Canada: Canadian Journal of Earth Sciences, v. 16, p. 792–807.

Williamson, T.C., 1996, BHP Minerals Canada Limited report on drilling, Eel River Group, 21-G/13: New Brunswick Department of Natural Resources, Minerals, Policy and Planning Division, Mineral Assessment report 474820, 61 p.

Winchester, J.A., and Floyd, P.A., 1977, Geochemical discrimination of different magma series and their differentiation products using immobile elements: Chemical Geology, v. 20, p. 325–343.